Knockdown of PHOX2B in the retrotrapezoid nucleus reduces the central CO_2 chemoreflex in rats.

Silvia Cardani [*1,2], Tara A. Janes [*1,2], William Betzner[1§], Silvia Pagliardini[#1,2,3]

[1]Department of Physiology, Faculty of Medicine and Dentistry, University of Alberta, Edmonton AB T6G2E1 Canada,

[2]Women and Children's Health Research Institute, University of Alberta, Edmonton AB T6G2E1 Canada.

[3]Neuroscience and Mental Health Institute, University of Alberta, Edmonton AB T6G2E1 Canada.

*SC and TAJ contributed equally to this work

[§] Current address: Departments of Clinical Neurosciences and Community Health Sciences, Hotchkiss Brain Institute, University of Calgary Cumming School of Medicine, Calgary AB T2N 4N1

[#]Corresponding author: Silvia Pagliardini, Department of Physiology, Faculty of Medicine & Dentistry, University of Alberta, 3020F Katz Group- Rexall Centre

Email: silviap@ualberta.ca.

Acknowledgments/ Author contributions

Concept and experimental design, S.P. and S.C.; Data collection, S.C., W.B. and S.P.; Data analysis, S.C. and T.A.J.; Manuscript preparation, S.C., T.A.J. and S.P.

S.C. is supported by the Canadian Lung Association BaO Fellowship. T.A.J. is supported by the Canadian Institutes for Health Research (CIHR) Postdoctoral Fellowships. S.P. is supported by a Women and Children's Health Research Institute Innovation Grant and CIHR Project scheme grant.

ABSTRACT

PHOX2B is a transcription factor essential for the development of the autonomic nervous system. Heterozygous mutations in the PHOX2B coding region are responsible for the occurrence of Congenital Central Hypoventilation Syndrome (CCHS), a rare neurological disorder characterised by inadequate chemosensitivity and life-threatening sleep-related hypoventilation. Animal studies suggest that chemoreflex defects are caused in part by the improper development or function of PHOX2B expressing neurons in the retrotrapezoid nucleus (RTN), a central hub for CO_2 chemosensitivity.

Although the function of PHOX2B in rodents during development is well established, its role in the adult respiratory network remains unknown. In this study, we investigated whether reduction in PHOX2B expression in chemosensitive neuromedin-B (NMB) expressing neurons in the RTN altered respiratory function. Four weeks following local RTN injection of a lentiviral vector expressing the short hairpin RNA (shRNA) targeting *Phox2b* mRNA, a reduction of PHOX2B expression was observed in *Nmb* neurons compared to both naïve rats and rats injected with the non-target shRNA. PHOX2B knockdown did not affect breathing in room air or under hypoxia, but ventilation was significantly impaired during hypercapnia. PHOX2B knockdown did not alter *Nmb* expression but reduced the expression of both *Task2* and *Gpr4*, two CO_2 sensors in the RTN. We conclude that PHOX2B in the adult brain has an important role in CO_2 chemoreception and reduced PHOX2B expression in CCHS beyond the developmental period may contribute to the impaired central chemoreflex function.

INTRODUCTION

The Paired Like Homeobox 2B (PHOX2B) is a transcription factor essential for embryonic differentiation and for the maintenance of the neuronal phenotype of different classes of neurons in both the central and peripheral nervous systems (Brunet & Pattyn, 2002; Pattyn et al., 1997, 1999, 2000; Stanke et al., 1999; Tiveron et al., 1996). In recent years, the PHOX2B gene has been extensively investigated, not only for its neurodevelopmental role, but also because its heterozygous mutation leads to Congenital Central Hypoventilation Syndrome (CCHS, OMIM 209880; Amiel et al., 2003), Hirschsprung's disease (HSCR; OMIM 142623; Berry-Kravis et al., 2006; Trochet et al., 2005), and neuroblastoma (Bourdeaut et al., 2005; Van Limpt et al., 2004). CCHS is a rare (1:200,000 births in France (Trang et al., 2005) and 1:148,000 births in Japan (Shimokaze et al., 2015) disorder characterised by a failure to respond to both hypercapnia and hypoxia (Amiel et al., 2003; Di Lascio et al., 2021; Weese-Mayer et al., 2017). The most frequent PHOX2B mutation is an expansion of a polyalanine repeat, ranging from +5 to +13 residues on the C-terminal of PHOX2B, an area that regulates DNA binding affinity and protein solubility (Amiel et al., 2003; Di Lascio et al., 2016; Weese-Mayer et al., 2003). CCHS symptoms present with varying degrees of severity depending on the expansion of the mutation (Berry-Kravis et al., 2006; Di Lascio et al., 2018; Matera, 2004). In most mild cases, patients display normal ventilation during wakefulness, hypoventilation during sleep leading to hypercarbia and hypoxemia, as well as a lack of sensitivity and discomfort to these challenges. In the most severe of cases, hypoventilation may also be present while awake.

Respiratory disturbances resulting from the PHOX2B mutations appear to stem from its widespread expression in respiratory-related neurons both during development and into adulthood. Although PHOX2B is absent in respiratory rhythmogenic neurons of the preBötzinger

complex, it is highly expressed in adult neurons that are responsible for CO_2 and O_2 chemoreflexes (Kang et al., 2007). Among those are the neurons of the retrotrapezoid nucleus (RTN), the locus coeruleus, the carotid bodies and the nucleus of the solitary tract that, together with the dorsal motor nucleus of the vagus nerve and the area postrema, make up to the dorsal vagal complex, a structure that provides the major integrative centre for the mammalian autonomic nervous system (Cutsforth-Gregory & Benarroch, 2017; Guyenet et al., 2019; Kang et al., 2007; Zoccal et al., 2014). Previous work by our group and others specifically investigated the role of PHOX2B-expressing RTN neurons by either selective lesions or inactivation of neuronal activity of these neurons (Abbott et al., 2011; Basting et al., 2015; Marina et al., 2010; Nattie & Li, 1994; Souza et al., 2018, 2023; Janes et al., 2024) and showed that RTN neurons have a key role in central CO_2 chemoreception.

Defects observed in the CO_2-chemoreflex of CCHS transgenic rodent models are primarily caused by the improper development or function of PHOX2B-expressing neurons in the RTN (Dubreuil et al., 2008; Ramanantsoa et al., 2011), although anatomo-pathological studies in CCHS patients suggest that the respiratory impairment may be caused by a more widespread brain dysfunction (Harper et al., 2015; Nobuta et al., 2015). Transgenic mice born with PHOX2B knockout fail to develop the RTN, the locus coeruleus (Pattyn et al., 1999) and catecholaminergic groups in A1, A2, A5 and A7 (Pattyn et al., 2000), as well as neurons of the nucleus of the solitary tract and the carotid bodies. Mice harbouring heterozygous PHOX2B knockout develop apparently normal but have depressed responses to hypoxia and hypercapnia (Dauger, 2003) and sleep disordered breathing in the perinatal period (Durand et al., 2005). Furthermore, the expression of the most common heterozygous PHOX2B mutation found in CCHS patients (PHOX2B +7Ala expansion) in mice resulted in a near complete loss of RTN neurons, impaired CO_2 response and consequent

98 death in the newborn period (Dubreuil et al., 2008; Madani et al., 2021; Ramanantsoa et al., 2011;
99 Takakura et al., 2008). More selective expression of the mutant PHOX2B in the RTN neurons
100 allowed for survival in the neonatal period and partial recovery of the CO_2 response in adulthood
101 (Ramanantsoa et al., 2011).
102
103 Multiple potential cellular mechanisms have been implicated in the etiology of CCHS, from loss of
104 PHOX2B function in development due to heterozygous mutant PHOX2B expression, to gain of
105 function of the mutated protein that may alter transcriptional activity in neurons, as well as
106 aggregate formation and premature cell death (Bachetti et al., 2005; Di Lascio et al., 2013;
107 Dubreuil et al., 2008; Durand et al., 2005; Goridis et al., 2010; Trochet et al., 2005). While its role
108 during embryonic neurodevelopment is established, PHOX2B is still expressed in selected neuronal
109 populations in the adult brain (Kang et al., 2007; Stornetta et al., 2006) and its function, with the
110 exception of the contribution to the maintenance of the noradrenergic phenotype (Fan et al.,
111 2011), is not yet fully understood. Considering the fundamental role of PHOX2B in CCHS
112 pathogenesis and its expression in key structures for CO_2 chemoreflex responses, it is essential to
113 understand how both wild-type and mutant PHOX2B proteins impact CO_2 homeostasis and
114 ventilation not only across development, but also in adulthood.
115 In order to have a better understanding of the role of PHOX2B in the CO_2 homeostatic processes
116 we used a non-replicating lentivirus vector of two short-hairpin RNA (shRNA) clones targeting
117 selectively *Phox2b* mRNA to knockdown the expression of PHOX2B in the RTN of adult rats and
118 tested ventilation and chemoreflex responses. In parallel, we also determined whether
119 knockdown of PHOX2B in adult RTN neurons negatively affected cell survival. Finally, we sought to
120 provide a mechanistic link between PHOX2B expression and the chemosensitive properties of RTN
121 neurons, which have been attributed to two proton sensors, the proton-activated G protein-

122 coupled receptor (GPR4) and the proton-modulated potassium channel (TASK-2) (Gestreau et al.,
123 2010; Guyenet et al., 2016; Kumar et al., 2015). The expression of these sensors is partially
124 overlapping in RTN neurons and the genetic deletion of either impairs the central respiratory
125 chemoreflex with maximal impairment when both sensors are eliminated (Gestreau et al., 2010;
126 Guyenet et al., 2016; Kumar et al., 2015).
127 Our results indicate that progressive knockdown of PHOX2B in RTN causes a reduction in the
128 chemoreflex response that was proportional to the decrease in the fraction of *Nmb*/PHOX2B
129 expressing RTN neurons. This effect was associated with a reduction in the expression of *Gpr4* and
130 *Task2* mRNA in *Nmb* expressing cells in which PHOX2B was knocked down, suggesting a role for
131 PHOX2B in the transcription of the proton sensors in RTN neurons.
132

133 **RESULTS**

134

135 To directly investigate the role of PHOX2B in RTN neurons, we performed selective knockdown of
136 this protein in adult rats through local injection of a non-replicating lentiviral vector of two short-
137 hairpin RNA (shRNA) clones targeting two different sequences of the *Phox2b* mRNA (n=25) or non-
138 target shRNA as control (NT-shRNA; n=23). Initial experiments utilized 200 nl/injection at each of 4
139 stereotaxic coordinates ($1x10^9$ VP/ml; n=14). Four weeks post injection, we assessed ventilatory
140 parameters in room air, hypercapnia, and hypoxia. Interestingly, a small but significant impairment
141 in the CO_2 chemoreflex was observed not only in PHOX2B-shRNA but also in NT-shRNA rats.
142 Specifically, room air breathing was not affected by RTN injection, but allometric V_E during 7% CO_2
143 was blunted in both NT-shRNA and PHOX2B-shRNA rats when compared to pre-surgical baseline (-
144 21% and -24%, respectively; Supp. Fig. 1A). Analysis of the air convection requirement ratio (CRR;
145 V_E/VO_2) confirmed that chemoreflex impairment during 7% CO_2 exposure was of central origin and

146 not due to lowered metabolism (data not shown). Given that CO_2 chemoreflexes were impaired in
147 both NT-shRNA and PHOX2B-shRNA rats, and histological analysis showed significant reduction of
148 *Nmb*$^+$/PHOX2B$^+$ RTN cells in NT-shRNA and PHOX2B-shRNA rats (33% and 19% cells remaining,
149 respectively; Suppl. Fig. 1), we concluded that the volume and titre of the shRNA viral constructs
150 triggered off-target effects (Mcbride et al., 2008; Van Gestel et al., 2014) that cause cell death in
151 RTN neurons.

152

153 **PHOX2B expression is modestly reduced two weeks following infection without respiratory**
154 **impairment.**

155 Due to the off-target effects obtained with large volume injections, we reduced injection volume
156 of both PHOX2B shRNA (n=17) and NT-shRNA viruses (n=17) (4x100nl/injection; $1x10^9$ VP/ml).

157 Two weeks post-surgery we assessed respiratory function during exposure to room air,
158 hypercapnia and hypoxia. Overall, we observed little change in respiration at this time point.
159 During room air, as well as in 5% and 7.2% CO_2, frequency (f_R), was reduced in every experimental
160 group (naïve, NT-shRNA, PHOX2B-shRNA) compared to baseline (Air: $p=0.014$; 5% CO_2: $p< 0.001$;
161 7.2% CO_2 $p< 0.001$; Fig. 1A) but no effect on treatment was observed, suggesting that these
162 changes were likely due to the increase in age and body weight during the experiment (naïve:
163 +32.2%; NT-shRNA: +27.8%; PHOX2B-shRNA: +28.6% body weight). Tidal volume was reduced in
164 the PHOX2B-shRNA rats at 7.2% CO_2 compared to both naïve rats (naive: 9.6 ± 1.2 $ml{\cdot}kg^{-1}$;
165 PHOX2B-shRNA: 8.5 ± 0.9 $ml{\cdot}kg^{-1}$; -11%; $p= 0.022$) and baseline conditions (baseline shRNA: 9.6 ±
166 1.3 $ml{\cdot}kg^{-1}$; -11%; $p< 0.001$; Fig. 1B) but it was not different from NT-shRNA.

167 Despite similar changes in body weight across treatment groups, allometric ventilation (V_E ALLO)
168 was increased in naïve rats compared to the other treatment groups in room air (naïve: 38.4 ± 4.5

169 ml·min^{-1}; NT-shRNA: 34.7 ± 2.8 ml·min^{-1}; PHOX2B-shRNA: 34.0 ± 4.5 ml·min^{-1}; p=0.005; Fig. 1C), but
170 no changes in V_E ALLO were observed in hypercapnia (7.2% CO_2) across treatments (naïve : 91.5 ±
171 13.2 ml·min^{-1}; NT-shRNA: 84.4 ± 13.7 ml·min^{-1}; PHOX2B-shRNA: 80.5 ± 17.2 ml·min^{-1}). Oxygen
172 consumption (VO_2 ALLO) was not different between experimental conditions or treatment groups
173 (Fig. 1D), and V_E/VO_2 ALLO indicated that ventilation was matched with metabolism for each
174 treatment across all gas compositions (naïve: 7.7 ± 1.3; NT-shRNA: 7.2 ± 1.3; PHOX2B-shRNA: 6.9 ±
175 2.0; Fig. 1E;). These results suggest that despite a reduction in hypercapnic V_T in the PHOX2B-
176 shRNA rats, overall ventilation was not impaired. Since we observed differences in room air V_E
177 ALLO between treatment groups, we normalized these data to show the hypercapnic ventilatory
178 response (HCVR, i.e., absolute change from room air; Fig. 1F). The HCVR was not affected by the
179 PHOX2B shRNA treatment two weeks post-injection (naïve: 53.1 ± 13.4 ml·min^{-1}; NT-shRNA: 49.6 ±
180 13.2 ml·min^{-1}; PHOX2B-shRNA: 46.5 ± 14.8 ml·min^{-1}).

181 To determine the extent of PHOX2B knockdown in RTN neurons we combined RNAScope® and
182 immunohistochemistry assays to quantify RTN neurons expressing *Nmb* and PHOX2B (Fig. 2B). We
183 reasoned that by assessing the fraction of RTN neurons that express only *Nmb* (compared to
184 *Nmb*$^+$/PHOX2B$^+$), we would be able to determine the level of PHOX2B knockdown in our
185 experiments. Two weeks post viral injection, we observed a significant decrease (15.2%) in the
186 total number of *Nmb*$^+$ RTN neurons (i.e., *Nmb*$^+$/PHOX2B$^+$ plus *Nmb*$^+$/ PHOX2B$^-$) in NT-shRNA rats
187 compared to naïve rats (naïve; 337.6 ± 11.95; n=4; NT-shRNA: 286.0 ± 10.44; n=4; p<0.001; Fig.
188 2C). The total number of *Nmb*$^+$ RTN neurons in PHOX2B-shRNA ratswas reduced compared to
189 naïve rats (PHOX2B-ShRNA 218.8 ± 7.8 n=4; -35.2%; p<0.001) and compared to NT-shRNA (-23.5%;
190 p<0.001).

191 In order to assess PHOX2B knockdown, we then quantified the number of neurons expressing
192 either *Nmb* and PHOX2B (*Nmb*$^+$/PHOX2B$^+$) or *Nmb* only (*Nmb*$^+$/PHOX2B$^-$). The number of

193 *Nmb*$^+$/PHOX2B$^+$ neurons in PHOX2B-shRNA rat was reduced by 36.1 % compared to NT-shRNA and
194 by 46.2% compared to naïve rats (*Nmb*$^+$/PHOX2B$^+$ NT-shRNA: 232.3 ± 11.6 vs naïve: 275.8 ± 17.1;
195 vs PHOX2B-shRNA: 148.3 ± 12.6; $p<0.05$ and 0.001, respectively; Fig. 2C,D). On the contrary, the
196 fraction of *Nmb*$^+$/PHOX2B$^-$ neurons in PHOX2B-shRNA rat was not different compared to naïve and
197 NT-shRNA rats (*Nmb*$^+$/PHOX2B$^-$ NT-shRNA: 53.7 +- 8.6; vs naïve: 61.8 +-13.9; vs PHOX2B-shRNA:
198 70.5 +- 8.7 cells; Fig. 2C,E). These results thus indicate that despite modest loss of *Nmb*$^+$ neurons in
199 NT-shRNA and PHOX2B-shRNA treated rats and nearly 50% reduction of *Nmb*$^+$/PHOX2B$^+$ in
200 PHOX2B-shRNA rats, 2 weeks of shRNA viral infection was not sufficient to impair ventilation.

201 **Four weeks of PHOX2B knockdown impairs the CO_2-chemoreflex.**

202 Since the shRNAs integrate into the genome of the infected cells and are continuously produced, it
203 is reasonable to expect that knockdown efficiency is time-dependent, and an extended infection
204 time would result in a higher knockdown effect. To test this hypothesis, a subgroup of rats (naïve,
205 NT-shRNA and PHOX2B-shRNA) were investigated four weeks post-viral injection (Fig. 3A,B).

206 The total number of RTN neurons in PHOX2B-shRNA rats (*Nmb*$^+$/PHOX2B$^+$ plus *Nmb*$^+$/PHOX2B$^-$; Fig.
207 3C) was significantly reduced compared to naïve rats (naïve: 347.8 ± 12 cells, n=4; PHOX2B-shRNA:
208 249.5 ± 33.9 cells; n=6; -28.3%; p=0.009) but no difference was observed compared to NT-shRNA
209 rats (294.9 ± 52.8 cells; n=10; -15.4%;). Furthermore, there was no difference in the total number
210 of *Nmb*$^+$ cells in RTN between 2 and 4 weeks post infection for both NT-shRNA (week 2: 286 ±
211 10.4; week 4: 294.9 ± 52.8, p=0.783) and PHOX2B-shRNA rats (week 2: 218.8 ± 7.8; week 4: 249.5
212 ± 33,9, p=0.118), suggesting that progressive PHOX2B knockdown was not accompanied by
213 increased cell death.

214 The number of PHOX2B expressing *Nmb*$^+$ cells in the RTN was significantly reduced in PHOX2B-
215 shRNA rats by 67.0% and 60.7% compared to naïve and NT-shRNA rats, respectively (naïve: 284.5 ±

216 19.8; NT-shRNA: 238.7 ± 56; PHOX2B-shRNA: 93.8± 11.9 cells, p<0.001; Fig. 3D). Moreover, a
217 significant increase in the fraction of *Nmb*$^{+}$/PHOX2B^{-} was observed with PHOX2B knockdown
218 (PHOX2B-shRNA: 155.7 ± 22.7; naïve: 63.2 ± 12cells; + 146.1% increase vs naïve; NT-shRNA: 56.2 ±
219 13.8cells; + 177% increase vs NT-shRNA, p<0.001; Fig. 3E).

220 The respiratory function prior to histological examination (4 weeks post-viral injection) showed
221 significant differences in PHOX2B-shRNA rats compared to both baseline, naïve and NT-shRNA
222 rats. Similar to what we reported at 2 weeks post-surgery, f_R at 4 weeks was significantly lower in
223 every treatment group compared to baseline recordings (Air: p=0.001; 5% CO_2: p< 0.001; 7.2% CO_2
224 p< 0.001; Fig. 4A).

225 During room air, V_T was modestly reduced in naïve rats compared to baseline (baseline: 5.9 ± 0.5
226 ml·kg^{-1}; week 4: 5.2 ± 0.6 ml·kg$^{-1;}$ -12%; p=0.001; Fig. 4B). Moreover, V_T in PHOX2B-shRNA rats was
227 reduced compared to NT-shRNA (NT-shRNA: 5.6 ± 0.4 ml·kg^{-1}; PHOX2B-shRNA: 5.3 ± 0.4 ml·kg^{-1}; -
228 10%; p=0.043) and to the baseline (6.1 ± 0.7 ml·kg^{-1}; -18%; p=0.002). No significant changes were
229 observed at 5% CO_2 although a decrease in V_T occurred at 7.2% CO_2 in PHOX2B-shRNA rats
230 compared to baseline pre-surgery (baseline: 7.7 ± 1.2 ml·kg^{-1}; PHOX2B-shRNA: 6.7 ± 0.6 ml·kg^{-1}; -
231 31%; p<0.001), naïve rats (7.9 ± 0.9 ml·kg^{-1}; -26%; p<0.001), and NT-shRNA rats (8.1 ± 0.7 ml·kg^{-1}; -
232 23%; p=0.002).

233 Decreased V_T observed for PHOX2B-shRNA led to a ventilation (V_E ALLO) impairment during
234 exposure to hypercapnia (7.2% CO_2, PHOX2B-shRNA vs. NT-shRNA: -17%; p=0.021; PHOX2B-shRNA
235 vs. naïve; -21% ; p=0.007; PHOX2B-shRNA vs. baseline, -18% p=0.002; Fig. 4C). Since O_2-
236 consumption (VO_2 ALLO) did not change (data not shown) a significant reduction in V_E/VO_2 ALLO
237 confirmed alveolar hypoventilation in PHOX2B-shRNA animals compared to NT-shRNA rats both at
238 5% (NT-shRNA: 5.8 ± 0.5; PHOX2B-shRNA: 4.8 ± 0.4; -16%; p=0.023) and 7.2% CO_2 (NT-shRNA: 7.9 ±
239 1.2; PHOX2B-shRNA: 6.1 ± 0.8; -24%; p=0.004; Fig. 4D). Moreover, the HCVR (normalized to room

240 air; Fig. 4E) at 7.2% CO_2 was lower in PHOX2B-shRNA (40.3 ± 9.4 ml·min^{-1}) rats compared to the
241 pre-surgery baseline (58.1 ± 8.9 ml·min^{-1}; -31%; p=0.015), naïve rats (63.6 ± 14.3 ml·min^{-1}; -37%;
242 p=0.008) and NT-shRNA rats (56.0 ± 10.4 ml·min^{-1}; -28%; p=0.016). Analysis of individual rats in
243 each treatment group over time showed that the HCVR was only consistently impaired in PHOX2B-
244 shRNA rats between weeks 2 and 4 (Fig. 1F; p=0.007).
245 Given that previous studies have proposed a role for the RTN in the hypoxic chemoreflex (Barna et
246 al., 2016; Basting et al., 2015; Gourine et al., 2005; Wickström et al., 2004), and we observed
247 impairment of the CO_2-chemoreflex at 4 weeks post-infection, we investigated whether PHOX2B
248 knockdown would also affect respiratory response to hypoxia (10% O_2). The 4 week V_E ALLO was
249 increased relative to baseline values in naïve (baseline: 62.3 ± 5.2 ml·min^{-1}; naïve: 71.0 ± 10.1
250 ml·min^{-1}; +14%), NT-shRNA (baseline: 71.8 ± 11.1 ml·min^{-1}; NT-shRNA: 75.8 ± 12.8 ml·min^{-1}; +6%)
251 and PHOX2B-shRNA rats (baseline: 65.9 ± 9.8 ml·min^{-1}; PHOX2B-shRNA: 79.3 ± 6.4 ml·min^{-1}; +29%;
252 p<0.001). However, analysis of the convective requirement ratio (V_E/VO_2 ALLO) indicates that
253 changes in hypoxic ventilation were due to metabolic adjustments that occurred in all treatment
254 groups (VE/VO_2 ALLO naive: 6.5 ± 1.3; NT-shRNA: 6.7 ± 1.7; PHOX2B-shRNA: 6.6 ± 0.6), suggesting
255 that the hypoxic ventilatory response was not affected by PHOX2B knockdown.

256

257 **PHOX2B knockdown does not extend to C1 catecholaminergic neurons and does not affect**
258 **mRNA expression of *Nmb* in RTN neurons**

259 Our data shows that PHOX2B knockdown specifically impairs breathing during hypercapnia. To
260 exclude that the observed impairment was due to unintended knockdown of PHOX2B in adjacent
261 areas of the brain, we quantified the total number of TH^+/PHOX2B$^+$ catecholaminergic C1 neurons
262 located caudal to the RTN in PHOX2B-shRNA rats compared to naïve and NT-shRNA (Fig. 5A). No
263 differences were observed in either the TH^+ cell numbers or in the PHOX2B expression between

264 the 3 treatment groups (naïve: 378.3 ± 23.81; NT-shRNA: 391.7 ± 33.08; PHOX2B-shRNA: 370.2 ±
265 33.04 cells).

266 NMB is currently considered the most selective anatomical marker for chemosensitive RTN
267 neurons (Shi et al., 2017) and was used in this study to identify RTN location, cell numbers and
268 relative PHOX2B expression. Since changes in the level of the transcription factor PHOX2B could
269 regulate the expression of its target genes, we investigated whether NMB is affected by shRNA
270 knockdown and assessed *Nmb* expression in PHOX2B-shRNA rats compared to both naïve and NT-
271 shRNA rats (Fig 5B). *Nmb* mRNA expression at the level of RTN was calculated as total fluorescence
272 intensity (CTCF) ratio relative to *Nmb* expression at the level of NTS, which served as an internal
273 control (Fig. 5B). We observed no changes in relative fluorescence of *Nmb* in RTN neurons across
274 the 3 groups (p=0.608), suggesting that NMB expression is not affected by PHOX2B knockdown.

275 To better analyse the association between PHOX2B knockdown in RTN neurons and the
276 attenuation of the HCVR, we evaluated the correlation between the number of Nmb^+/PHOX2B$^+$ or
277 Nmb$^+$/PHOX2B$^-$ cells in the RTN and the resulting HCVR using linear regression (Fig. 5C,D). Our
278 results indicate that there is a significant correlation between HCVR and number of
279 Nmb$^+$/PHOX2B$^+$ (r^2 = 0.739 p<0.001; Fig. 5C), and Nmb$^+$/PHOX2B$^-$ (r^2 = 0.482 p<0.001 Fig. 5D) cells
280 suggesting that the number of PHOX2B expressing cells in the RTN is a good predictor of the
281 chemoreflex response. Moreover, the nature of the correlation between PHOX2B$^-$ cells and HCVR
282 is the opposite of PHOX2B$^+$, another important indicator that PHOX2B protein contributes to the
283 CO_2 sensing and consequently, the reduction of PHOX2B protein impairs the CO_2-chemoreflex.

284

285 **Gpr4 and Task2 mRNAs expression is affected by PHOX2B Knockdown**

286 We next examined the mRNA expression of *Gpr4* and *Task2*, two important pH sensors for the
287 central respiratory chemoreflex response in RTN neurons (Gestreau et al., 2010; Guyenet et al.,
288 2016; Kumar et al., 2015). As previously reported, the two pH sensors are expressed in the NMB
289 RTN neurons in partially overlapping populations of chemosensory neurons (Gestreau et al., 2010;
290 Kumar et al., 2015). In naïve rats 91.6 ± 11.2 % of NMB cells were *Gpr4* positive, and 76.6 ± 14.8 %
291 of NMB cells were also *Task2* positive (n=4 rats). These values were not significantly different in
292 either NT-shRNA or PHOX2B shRNA rats (NT-shRNA: 90.0 ± 15.7% $Nmb^+/Gpr4^+$ and 76.2 ± 21.8%
293 $Nmb^+/Gpr4^+$, n=10 rats; PHOX2B-shRNA: 89.4 ± 18.3% $Nmb^+/Gpr4^+$ and 75.6 ± 27.8% $Nmb^+/Gpr4^+$,
294 n=6 rats).

295 To further investigate whether the expression of these two sensors was affected by the reduction
296 in PHOX2B protein we quantified the total fluorescence intensity (CTCF) for their mRNA in Nmb^+
297 cells. Total CFCT for *Gpr4* and *Task2* in PHOX2B-shRNA rats was significantly reduced compared to
298 naïve and NT-shRNA rats (*Gpr4*: -34.4 ± 4.79% vs naïve, -27.9 ± 5.71% vs NT-shRNA $p<0.001$; *Task2*:
299 -39.0 ± 3.02% vs naïve, -34 ± 2.62% vs NT-shRNA $p<0.001$; Fig. 6B,D). To better understand
300 whether this reduction was ascribed to the specific loss of PHOX2B expression, we compared the
301 mRNA expression levels between Nmb^+/PHOX2B$^-$ and Nmb^+/PHOX2B$^+$ neurons in PHOX2B-shRNA
302 rats. Both *Gpr4* and *Task2* mRNA expression was reduced in Nmb^+/PHOX2B$^-$ cells compared to
303 Nmb^+/PHOX2B$^+$ (*Gpr4*: -63.8 ± 3.9%; p= 0.022; *Task2*: -63.2 ± 2.77%; p= 0.029; Fig. 6C,E). Our data
304 suggest that PHOX2B knockdown not only causes a reduction in the hypercapnic respiratory
305 response but also a reduction in the expression of *Gpr4* and *Task2* mRNAs.

306

307

308 **DISCUSSION**

309

310 The role of the transcription factor PHOX2B in the adult brain is still not fully understood. In this
311 study we reduced the expression of PHOX2B in the key chemosensory structure of the RTN with a
312 selective viral shRNA approach to test whether a knockdown of PHOX2B expression in these
313 neurons negatively impacts ventilation. Two weeks after viral infection we observed a modest
314 reduction of PHOX2B/NMB expressing neurons in the RTN but no significant changes in basal V_E or
315 in the CO_2 chemoreflex. Four weeks after shRNA infection we observed a further reduction in the
316 expression of PHOX2B in RTN neurons and a significant reduction of the CO_2 chemoreflex, while
317 ventilation in normoxia or hypoxia was unaffected. Furthermore, the level of expression of *Gpr4*
318 and *Task2* mRNA, the two proton sensors responsible for the RTN neurons chemosensory
319 properties were significantly reduced in RTN neurons that lacked PHOX2B protein expression,
320 whereas *Nmb* mRNA expression level was unaffected by PHOX2B knockdown. These results
321 suggest that PHOX2B reduction affects RTN neurons transcriptional activity and decreases the CO_2
322 response, possibly by reducing the expression of key proton sensors in the RTN.

323 **The role of PHOX2B in development and in the adult brain**

324

325 PHOX2B is a transcription factor with an important role in the development and differentiation of
326 neuronal structures in both the central and peripheral nervous system. Genetic loss of PHOX2B
327 expression in mice shows that PHOX2B is essential for the correct development of all autonomic
328 ganglia in sympathetic, parasympathetic, and enteric nervous system and the distal ganglia of the
329 facial (VII), glossopharyngeal (IX), and vagus (X) cranial nerves (Pattyn et al., 1999), in addition to
330 carotid bodies and the solitary tract nucleus (Dauger, 2003). Furthermore, PHOX2B is involved in
331 the formation of all branchial and visceral hindbrain motor neurons and its absence during
332 embryonic period impairs the development of motoneurons of the facial, trigeminal, ambiguus

333 and dorsal motor nucleus of the vagal nerve. PHOX2B is also necessary for the specification and
334 differentiation of the noradrenergic phenotype in multiple centres in the brain (Brunet & Pattyn,
335 2002; Pattyn et al., 1999, 2000a).
336 Interestingly, the expression of PHOX2B persists into adulthood in selected neuronal populations,
337 such as the ones involved in peripheral and central chemoreception, i.e., the carotid bodies, the
338 solitary tract nucleus and the RTN, in addition to neurons in the dorsal motor nucleus of the vagus,
339 the area postrema, the nucleus ambiguus, C1 catecholaminergic neurons and other scattered
340 neurons throughout the brainstem (Stornetta et al., 2006). Such widespread expression within the
341 adult brain suggests an important transcriptional role in neuronal survival and/or function. With
342 the exception of its role in maintaining the noradrenergic phenotype, its function in the postnatal
343 brain is unknown, in part because a full investigation of its transcriptional activity in vivo has not
344 yet been performed.
345 Heterozygote polyalanine expansion mutations in the exon 3 of *PHOX2B* are responsible for the
346 majority of cases of CCHS, a rare genetic disease that affect the autonomic nervous system and
347 central CO_2 chemoreflexes (Amiel et al., 2003; Di Lascio et al., 2021; Weese-Mayer et al., 2017).
348 While studies in transgenic mice expressing the mutated PHOX2B protein suggest that the RTN
349 may not form or be severely impaired (Dubreuil et al., 2008, 2009; Ramanantsoa et al., 2011), the
350 function of the wild-type protein in these neurons has never been tested in adulthood. Thus, in
351 order to determine whether PHOX2B is necessary for the survival and/or chemosensory function
352 of adult PHOX2B$^+$ RTN neurons in vivo, we used a shRNA viral approach to progressively
353 knockdown the PHOX2B protein in these neurons.
354
355 **Modest reduction of PHOX2B in RTN does not impair ventilation**
356 We identified RTN neurons by the mRNA expression of the neuropeptide, NMB (Shi et al., 2017)
357 and observed a reduced number in both total *Nmb*$^+$ and *Nmb*$^+$/PHOX2B$^+$ neurons in shRNA rats

358 compared to naïve and NT-shRNA rats two weeks after viral infection. Interestingly, despite the
359 small reduction in total *Nmb*$^+$ RTN neurons in both NT-shRNA and PHOX2B-shRNA injected rats,
360 possibly due to some off-target effects due to activation of innate immunity or saturation of the
361 microRNA pathway (Mcbride et al., 2008; Van Gestel et al., 2014), no significant impairment in
362 ventilation was observed. Nonetheless, the fraction of *Nmb*$^+$ cells expressing PHOX2B was reduced
363 indicating that shRNA knockdown occurred in a fraction of RTN neurons. Even though PHOX2B
364 may be critical for chemosensory function in RTN neurons, the lack of significant ventilatory
365 impairment with a modest reduction of PHOX2B expressing neurons is not surprising. In our
366 previous study (and the ones of others), in which RTN chemosensory neurons were lesioned with
367 Substance P saporin toxin, CO_2-chemoreflex impairment became significant (~30% V_E Allo
368 reduction vs. pre-surgical baseline) only when the sum of *Nmb*$^+$/PHOX2B$^+$ and *Nmb*$^+$/PHOX2B$^-$
369 neurons was reduced by ~63% compared to naïve controls (medium lesion range: 50%-81% loss of
370 *Nmb*$^+$ neurons; Janes et al., 2024; Souza et al., 2023), therefore, even though loss of PHOX2B
371 severely altered the chemosensitive function of NMB cells, we would not expect significant
372 changes in ventilation with a <50% RTN cell loss.
373

374 **Four weeks of PHOX2B knockdown impairs central CO_2 chemoreception**

375
376 Four weeks post- shRNA viral injection, the fraction of *Nmb*$^+$ cells expressing PHOX2B was further
377 reduced by 67% compared to naïve and by 61% compared to NT-shRNA rats. PHOX2B knockdown
378 was also restricted to RTN neurons, as more caudal C1 TH$^+$ neurons and the adjacent FN
379 motoneurons did not show any change in number or PHOX2B expression. Although we did not
380 specifically quantify the relative mRNA expression change in intracellular *Phox2b* levels within
381 infected neurons, we measured the success of PHOX2B knockdown by assessing the overall
382 change in the number of *Nmb*$^+$ cells that had no detectable levels of PHOX2B protein in the nuclei.

383 Thus, it is possible that this method led us to underestimate the success of the overall PHOX2B
384 shRNA knockdown in the RTN.
385 In PHOX2B-shRNA rats we did not observe any respiratory function changes in room air or in
386 hypoxia, similar to RTN lesioning studies (Janes et al., 2024; Souza et al., 2023). When tested in
387 hypercapnia though, PHOX2B-shRNA rats displayed a reduced HCVR compared to both baseline
388 (i.e., pre-surgery), naïve and NT-shRNA rats. The impairment of V_E Allo was primarily a result of
389 blunted V_T, and analysis of the convective exchange ratio (i.e. V_E/VO_2 ALLO) confirmed
390 hypoventilation in 5% and 7.2% CO_2 only for PHOX2B-shRNA rats, suggesting a specific impairment
391 of chemosensitive properties in RTN neurons with PHOX2B knockdown. These results are in line
392 with previous studies in which medium RTN lesions (i.e. loss of >60 % *Nmb*$^+$ cells) elicited by
393 Saporin toxin injection resulted in a significant CO_2-chemoreflex impairment (Janes et al., 2024;
394 Souza et al.,2018).
395 Changes in the CO_2 response following 4 weeks of PHOX2B-shRNA treatment could occur because
396 the reduced expression of the transcription factor PHOX2B causes changes in the transcriptional
397 machinery of RTN neurons and alters transcription of CO_2/pH sensing proteins or other key
398 elements for their chemosensitive function. These transcriptional changes could also affect
399 neuronal survival. In fact, a small but significant loss of NMB expressing RTN neurons may
400 contribute to the reduction in the CO_2 response, although multiple studies have demonstrated
401 that significant cell loss must occur in the RTN in order to show a respiratory function impairment
402 (Janes et al., 2024; Souza et al.,2018; Nattie & Li, 2002; Takakura et al., 2008, 2014).
403 In our experiments, we observed a 35% reduction in total *Nmb*$^+$ cells compared to naïve rats and
404 23% compared to NT-shRNA, possibly due to cell death within the first 14 days post-infection.
405 Interestingly the loss of *Nmb*$^+$ cells did not increase with time (although the number of PHOX2B$^+$
406 neurons decreased) and the central chemoreflex at 2 weeks post-surgery was not impaired,

407 suggesting that: i) the observed reduction in overall RTN cell number is not responsible for the CO_2
408 chemoreflex impairment; ii) PHOX2B expression is most likely not necessary for neuronal survival
409 of RTN neurons; iii) a large reduction in RTN PHOX2B$^+$ neurons is necessary to impair the HCVR.
410 The interpretation that PHOX2B expression contributes positively to the chemoreflex is further
411 supported by our linear regression analysis showing that *Nmb*$^+$/PHOX2B$^+$ cell number was the best
412 predictor of the HCVR (r^2 = 0.739). The initial cell loss, which we observed also in NT-shRNA, and
413 more prominently with larger injection volume of virus, may be attributed to some inherent cell
414 death associated with the surgical procedure or, more likely, with the potential off-target toxic
415 effects associated with shRNA procedures (Mcbride et al., 2008; Van Gestel et al., 2014).
416
417 **PHOX2B knockdown reduces expression of proton sensors in the RTN**
418 Current theories on central respiratory chemosensitivity postulate that changes in CO_2/pH in the
419 RTN are detected through two pH sensors, the proton-activated receptor GPR4 and the pH-
420 sensitive K^+ channel TASK2 that are expressed in partially overlapping populations of NMB
421 expressing RTN neurons (Kumar et al., 2015). Because it is not known whether PHOX2B has any
422 effect on the expression of TASK2, GPR4 or even the expression of the neuropeptide NMB used to
423 anatomically identify RTN neurons, we determined their mRNA levels within the RTN (calculated
424 as CFTC) and observed no changes in relative fluorescence of *Nmb*$^+$ mRNA in RTN neurons relative
425 to *Nmb* expression in unrelated cells in the NTS, suggesting that NMB is not affected by PHOX2B
426 shRNA knockdown and that *Nmb* is most likely not a target gene of PHOX2B in adult RTN neurons.
427 Furthermore, we determined the mRNA expression levels of *Task2* and *Gpr4* in both
428 *Nmb*$^+$/PHOX2B$^+$ and Nmb$^+$/PHOX2B$^-$ neurons in shRNA rats. Our results indicate that the total CTCF
429 for *Gpr4* and *Task2* in PHOX2B-shRNA rats was reduced compared to naïve and NT-shRNA group.
430 Furthermore, there was a significant reduction of both *Gpr4* and *Task2* in *Nmb*$^+$/PHOX2B$^-$ cells
431 compared to *Nmb*$^+$/PHOX2B$^+$ cells. Because no good antibodies are currently available to detect

432 protein levels of either NMB, GPR4 or TASK2, our results are only based on changes in mRNA
433 levels, thus we can only speculate that a reduction in *Gpr4* and *Task2* mRNA would translate in a
434 reduction in the protein levels and consequent reduction of RTN neurons chemosensitive
435 properties. Direct electrophysiological recordings in RTN neurons will be able to address the
436 changes in CO_2/pH sensitivity of RTN neurons at cellular level.
437
438 **PHOX2B knockdown may impair CO_2-sensing through additional transcriptional targets**
439 Since loss of PHOX2B reduces expression of TH and dopamine beta hydroxylase enzymes in
440 catecholaminergic neurons *in vivo* and *in vitro* (Fan et al., 2011), it is possible that in NMB^+ RTN
441 neurons, reduction of PHOX2B alters the transcriptional machinery of other proteins (in addition
442 to GPR4 and TASK2) and impairs their function in central chemoreception. For example, a change
443 in the expression of enzymes, neurotransmitters, receptors, and ion channels in RTN neurons
444 could affect the excitatory signal transmission to preBötzinger Complex and the respiratory
445 network specifically during CO_2 challenges (Guyenet et al., 2016). Further studies will be needed to
446 address and identify additional transcriptional changes induced by PHOX2B knockdown *in vivo.*
447 An interesting observation from our histological data was the reduction in the overall number of
448 *Nmb*$^+$ cells at two- and four-weeks following shRNA viral injections. Although some cell death may
449 be associated with either surgical procedures or off-target effects associated with the shRNA
450 approach (Mcbride et al., 2008; Van Gestel et al., 2014), it is intriguing to speculate that loss of
451 PHOX2B expression may have some effects on viability of RTN neurons *in vivo*. Even though this is
452 a possibility, especially with an even more severe knockdown, we did observe a large proportion
453 of *Nmb*$^+$ cells devoid of PHOX2B protein expression, suggesting that absence of PHOX2B is
454 compatible with neuronal survival, at least in our experimental time frame.
455
456 **Relevance to CCHS and its pathogenic mechanisms**

457 Our results contribute to further our understanding on potential pathogenic mechanisms in CCHS
458 (Di Lascio et al., 2018). Homozygous knockout mice for PHOX2B die during gestation (Pattyn et al.,
459 1999, 2000) demonstrating a key role of this transcription factor in cellular proliferation, migration
460 and differentiation during embryonic development, whereas heterozygotes for PHOX2B survive
461 birth and live into adulthood, but display apneas (Durand et al., 2005) and impairment of the
462 hypoxic and hypercapnic ventilatory responses in the neonatal period (Dauger, 2003). Here we
463 show that, independent of the PHOX2B role during development, PHOX2B is still required to
464 maintain proper CO_2 chemoreflex responses in the adult brain.
465 Heterologous expression of the mutant PHOX2B alters development of RTN in mice and impairs
466 their chemoreflex response (Dubreuil et al., 2008, 2009). The effects of the expression of the
467 mutant PHOX2B on wild-type PHOX2B and its transcriptional activity is not known *in vivo* yet,
468 although *in vitro* data indicates that the mutated PHOX2B protein alters wild-type PHOX2B
469 conformation and its ability to form homo- and hetero-dimers (Di Lascio et al., 2016; Trochet et
470 al., 2005, 2008), its affinity for DNA and coactivators, as well as its degradation rate (Nagashimada
471 et al., 2012; Wu et al., 2009). It has also been shown that mutant PHOX2B causes the formation of
472 cytoplasmic aggregates (Bachetti et al., 2005; Trochet et al., 2005, 2008) and fibrils *in vitro* (Pirone
473 et al., 2019), and dysregulates the transcriptional function of wild-type PHOX2B (Di Lascio et al.,
474 2013; Parodi et al., 2012), thus changing expression of important target genes such as DBH,
475 PHOX2A and TLX2 (Bachetti et al., 2005; Di Lascio et al., 2013; Trochet et al., 2005). Based on this
476 evidence, different CCHS pathogenic mechanisms have been proposed (e.g., PHOX2B loss-of-
477 function, dominant-negative or toxic function of the mutant protein) including gene and cell
478 specific transcriptional dysregulation (Di Lascio et al., 2018, 2021). Interestingly, only a handful of
479 PHOX2B target genes have been identified and the function of PHOX2B and its mutated forms in
480 respiratory control and CCHS pathogenesis is still under investigation.

481 Our data suggest that, in addition to potential effect of mutated PHOX2B on development and
482 cellular function in CCHS pathogenesis, the expression of wild type PHOX2B has an important role
483 in respiratory control that extends the developmental period and its reduction in CCHS may
484 contribute to the respiratory impairment in this disorder.

485

486 **MATERIALS AND METHODS**

487 Experiments were performed using male Sprague–Dawley rats (starting weight range 250-350g)
488 born in the University of Alberta animal facility to pregnant dams obtained from Charles River
489 (Senneville, QC). Rats were housed at the University of Alberta Health Sciences Animal Housing
490 Facility and maintained on a 12-hr dark/light cycle with food and water available *ad libitum*.
491 Handling and experimental procedures were approved by the Health Science Animal Policy and
492 Welfare Committee at the University of Alberta (AUP#461) and performed in accordance with
493 guidelines established by the Canadian Council on Animal Care.

494

495 **ShRNA viral injection in the retrotrapezoid nucleus**

496 In order to knockdown Phox2b expression at the level of RTN neurons, we used a mix of two
497 shRNA clones targeting two different sequences of the Phox2b mRNA carried by a non-replicating
498 lentivirus vector ($1x10^9$ VP/ml; TRCN000041283: GCCTTAGTGAAGAGCAGTATG and
499 TRCN0000096437: CCTCTGCCTACGAGTCCTGTA; Sigma Aldrich, St. Louis, MA, USA). The shRNAs
500 were designed against the Phox2b mouse sequence (Ref Seq NM_008888) which shares 100%
501 homology with the Phox2b rat sequence (Ref Seq XM_008770167).

502 Metacam analgesic was administered 1 hour prior to surgery (2mg/kg) to reduce post-surgical
503 pain. Rats were anesthetized with a ketamine/xylazine mixture (100mg/kg + 10mg/kg,
504 respectively; i.p.); the anaesthetic level was assessed by lack of paw pinch reflex and maintenance
505 of a regular breathing rate. Additional anaesthesia was administered as needed. The rat was
506 positioned on a stereotactic apparatus (Kopf Instruments, Tujunga, CA, USA) and a total of four
507 microinjections (200 or 100 nL per injection; two rostro-caudally aligned injections per side) were
508 made lateral to the midline and ventral to the facial motor nucleus under aseptic conditions.
509 Coordinates were as follows in mm from obex (medio-lateral/rostro-caudal/dorso-ventral): ±1.8,
510 +2.0,-3.5; ±1.8,+2.4,-3.6. Injections were made using a glass microelectrode (30 µm diameter tip,
511 Drummond Scientific, PA, USA). Twenty-five rats (8 rats 200nl/injection; 17 rats 100nl/injection)
512 underwent shRNA viral injection (PHOX2B-shRNA) and 23 rats (6 rats 200nl/injection; 17 rats
513 100nl/injection) received a non-target shRNA viral injection (NT-shRNA; SHC016:
514 MISSION® pLKO.1-puro non-Target shRNA Control Plasmid DNA; Sigma Aldrich, St. Louis, MA, USA)
515 to determine any effects of surgery alone on respiratory behaviour. Eight naïve rats, receiving no
516 surgery and maintained in the same housing conditions, were used as additional controls for both
517 respiratory function and anatomical experiments. Following each injection, the glass electrodes
518 were left in place for 3-5 minutes to minimize backflow of virus up the electrode track. At the end
519 of the surgery, the incision was sutured, and rats received local anaesthetic bupivacaine (0.1 mL,
520 s.c.) and were treated with metacam analgesic for 72 hours. Rats recovered for 7 days before the
521 next respiratory function testing.

522

523 **Data acquisition and analysis of respiratory measurements**

524 Rats were habituated to whole-body plethysmography chambers (Buxco, 5L) once, 3-4 days before
525 baseline recordings. On the day of the experiment, rats were placed in the chamber and testing

526 commenced once the animals were quietly awake (typically 20-30 mins). Gas mixtures were
527 delivered at 1.5 L/min using a GSM-3 (CWE Inc., Ardmore, PA, USA) and monitored using a Gas
528 Analyzer (AD Instruments, Sydney, Australia). Ventilatory parameters were measured during
529 exposure to different air compositions for 8-15 min each. Room air: 21%O_2 + 0%CO_2 (balanced
530 with N_2); Normoxic Hypercapnia: 21%O_2+ 5%CO_2; 21%O_2 + 7.2%CO_2; Normocapnic Hypoxia:
531 10.6%O_2+ 0% CO_2.

532 As previously described (Cardani et al., 2022; Janes et al., 2024) respiratory data were analysed
533 from rats during quiet wakefulness in the last 5 min period of each gas composition using the
534 barometric method (open-flow system) (Cardani et al., 2022; Janes et al., 2024; Mortola &
535 Frappell, 1998; Seifert et al., 2000). Raw pressure signals were acquired with a Validyne
536 differential pressure transducer connected to a CD15 carrier demodulator (Validyne Engineering,
537 Northridge, CA, USA) and digitized using a Powerlab 8/35 (AD Instruments, Sydney, Australia).
538 Analysis was done using Labchart 8 (v8.1.19, AD Instruments, Colorado Springs, CO, USA) to
539 determine tidal volume (V_T) and breathing frequency (f_R). The amplitude of the pressure signal was
540 converted to V_T (ml·kg^{-1}) using the equations of Drorbaug and Fenn 1955 (Drorbaugh & Fenn,
541 1955) and calibrated against 1 mL of dry air injected into the empty chamber using a rodent
542 ventilator (Harvard Rodent Ventilator Model 683, Holliston, MA, USA f = 50, 75, 100, 150
543 beats·min^{-1}). Humidity and chamber temperature were monitored using a RH-300 water vapour
544 analyzer (Sable Systems, Las Vegas, NV, USA) and a HPR Plus Handheld PIT Tag reader (Biomark,
545 Boise, ID, USA) respectively, depending on the setup. Rectal temperature was read through the
546 temperature probes of a Homeothermic Monitor (507222F, Harvard Apparatus, Holliston, MA,
547 USA). Minute ventilation ($\dot{V}_E$) was calculated as f_R x V_T and expressed as ml·min^{-1}·kg^{-1}. Rats gained,
548 on average, 160 ± 4g over the experimental paradigm (naive: 158 ± 19g ; NT-shRNA: 202 ± 25g ;

549 PHOX2B-shRNA: 133 ± 7g); we therefore applied an allometric correction to $\dot{V}_E$ to account for non-
550 linear effects of weight gain (V_E ALLO) (Mortola et al., 1994).

551 Metabolic parameters VO_2 and V_E/VO_2 were calculated by pull-mode indirect calorimetry and
552 allometerically scaled to be consistent with ventilation (Mortola et al., 1994). The % composition
553 of dry gas flowing into, and out of the recording chamber was measured by using an AD
554 Instruments Gas Analyzer (Colorado Springs, CO) and applying the equations of Depocas and Hart
555 (Depocas F, Hart JS, 1957) and Lighton (Lighton, 2021).

556 Weight measurements were taken prior to any recording. Rats breathing function was measured
557 the week prior to surgery (baseline recording) and weekly following shRNA injections to determine
558 the time course of ventilatory impairment.

559 Respiratory data were compared for naive, NT-shRNA and PHOX2B-shRNA pre- and post-injection
560 using a mixed factor ANOVA (independent factor = treatment, repeated measures factor = pre-
561 and post-lesion; Fig.1,4). Post-hoc analysis used the Bonferroni correction factor, with $p<0.05$
562 considered to be significant. Ventilatory data are reported as mean ± standard deviation (SD).

563

564 **In Situ hybridization (RNAScope) and immunofluorescence**

565 Either 2 or 4-weeks after viral injection, rats were transcardially perfused with saline 0.9% NaCl
566 followed by 4% paraformaldehyde (PFA) and the brains were post-fixed in 4% PFA overnight and
567 cryoprotected in 30% sucrose in 1X Phosphate Buffered Saline (PBS). Brains were then frozen in
568 O.C.T compound (Fisher Scientific) and sectioned on a cryostat (MODEL CM1950, Leica
569 Biosystems, Buffalo grove, IL, USA) at 30 µm and stored in cryoprotectant buffer at -20°C until
570 processing. Sections were mounted on slides for combined RNAScope® in situ hybridization
571 (Advanced Cell Diagnostics-ACD Bio, Newark CA, USA) and immunofluorescence assay and

572 processed as previously detailed (Biancardi et al., 2021; Cardani et al., 2022). The mRNA
573 expression for *Neuromedin B* (*Nmb)* was used as marker of RTN CO_2-sensing neurons (Shi et al.,
574 2017). Slides were incubated with probes for *Nmb* (Rn-NMB-C2 #494791-C2, ACDBio, Newark, CA,
575 USA), *Phox2b* (Rn-Phox2b-O1-C1 #1064121-C1, ACDBio), G-protein-coupled receptor 4 (*Gpr4*)
576 (Mm-Gpr4-C1, #427941, ACDBio), and potassium channel, subfamily K, member 5 (*Kcnk5* or *Task-*
577 *2*) (Mm-Kcnk5-C3, #427951-C3, ACDBio) for 2 hr at 40°C. Gpr4 and Kcnk5 probes are design against
578 the mouse mRNA sequence (Ref Seq NM_175668.4 and NM_021542.4, respectively). However,
579 the alignment of the mouse mRNA sequences with those of rat (GPR4: Ref Seq NM_001025680.1;
580 TASK2: Ref Seq NM_1039516.2) showed an identity of 94% and 96%, respectively, at the level of
581 the target region (Base Pairs 1030-150) (BLAST® program, National Library of Medicine, National
582 Center for Biotechnology Information, NIH). In parallel, two sections/rat were treated with
583 positive (low copy housekeeping gene), and negative (non-specific bacterial gene) control probes
584 provided by ACDBio. Finally, slides were processed using the RNAScope Multiplex Fluorescent
585 Assay kit V2 (ACDBio) according to the manufacturer's instructions. The probes were visualized
586 using Opal 520 and Opal 570 reagent (1:500 and 1:1000, respectively; PerkinElmer, Woodbridge,
587 ON, CA). PHOX2B immunoreactivity was detected using mouse monoclonal PHOX2B antibody (B-
588 11: sc-376997, 1:100, Santa Cruz Biotechnology) incubated overnight in 0.3% TritonX-100, 1%NDS
589 in PBS followed by donkey CY5-conjugated anti-mouse IgG (1:200; Jackson Immuno Research
590 Laboratories Inc) in PBS + 1% NDS for 2 hours. Slides were then washed in PBS and cover-slipped
591 with Fluorosave mounting media (EMD Millipore).

592 We also performed staining for tyrosine hydroxylase (TH) to identify and quantify C1 cells
593 (TH^+/$PHOX2B^+$) following shRNA injection. Briefly, perfusion and tissue fixation/freezing were done
594 as described above. Floating sections were stained with rabbit anti TH antibody (AB152,1:1000,
595 Millipore SIGMA, USA), and mouse anti PHOX2B (B-11: sc-376997, 1:100, Santa Cruz

596 Biotechnology). Antibodies were visualized using donkey CY3 (TH) and CY5 (PHOX2B) conjugated
597 IgG (1:200; Jackson Immuno Research Laboratories Inc). The sections were washed in PBS and
598 mounted on slides and cover-slipped with Fluorosave mounting media.

599

600 **Cell counting, imaging and data analysis.**

601 To quantify the number of neurons *Nmb*$^{+}$/PHOX2B^{-} *and Nmb*$^{+}$/PHOX2B^{+} within the RTN region, we
602 analysed one every 7 sections (210 µm interval; 8 sections in total; from -12.5 to -11.1 mm from
603 Bregma, according to the Paxinos and Watson atlas coordinates (Paxinos & Watson, 2023) and
604 compared total bilateral cell counts of PHOX2B-shRNA rats with non-target control (NT-shRNA)
605 and naïve rats. Cells that express *Nmb* and *Phox2b* mRNA but do not show co-localization with
606 PHOX2B protein were considered *Nmb*$^{+}$/PHOX2B^{-}.

607 The Correct Total Cell Fluorescence (CTCF) signal for *Nmb, Gpr4* and *Task2* mRNA was quantified
608 as previously described (Cardani et al., 2022; McCloy et al., 2014). A Leica TCS SP5 (B-120G) Laser
609 Scanning Confocal microscope was used to acquire images of the tissue. Exposure time and
610 acquisition parameters were set for the naïve group and kept unchanged for the entire dataset
611 acquisition. For each image, three background areas were used to normalize against
612 autofluorescence. We used 4 sections/rat to count *Nmb*, *Gpr4* and *Task2* mRNA CTCF in the RTN
613 area (-12.3 to -11.7 mm from Bregma). For each section two images were acquired with a 20×
614 objective, so that at least fifty cells per tissue sample were available for analysis. To evaluate
615 changes in *Nmb* mRNA expression following PHOX2B knockdown at the level of the RTN, we
616 compared, on the same tissue section, the fluorescence intensity of RTN *Nmb*$^{+}$ cells with the signal
617 of *Nmb*$^{+}$ cells in the NTS (*Nmb* CTCF ratio RTN/NTS) as the latter would not be affected by the
618 shRNA infection and knockdown.

619 To quantify *Gpr4* and *Task2* mRNA expression in the RTN, we first quantified CTCF for either *Gpr4*
620 or *Task2* mRNA in *Nmb*$^+$ RTN neurons in the 3 experimental groups. We then compared CTCF of
621 *Gpr4* and *Task2* mRNA between *Nmb*$^+$/PHOX2B$^+$ and *Nmb*$^+$/PHOX2B$^-$ RTN neurons in PHOX2B-
622 shRNA rats to address changes in mRNA expression induced by PHOX2B knockdown.

623 To assess whether shRNA knockdown affected either the number or the expression of PHOX2B in
624 C1 neurons, we counted the number of TH$^+$/PHOX2B$^+$ cells along the ventrolateral medulla (-13.2
625 to -11.5 mm from bregma; 8 sections/rat; 240 µm interval) using an EVOS fluorescent microscope
626 (ThermoFisher Scientific).

627 Digital colour photomicrographs were acquired using a Leica TCS SP5 (B-120G) Laser Scanning
628 Confocal microscope. Image J (version 1.54f; National Institutes of Health, Bethesda, MD, USA)
629 and Excel (Microsoft Office 365 for Windows) were used for cell counting and the measurements
630 of fluorescence intensity. Statistical analysis of cell counts, and fluorescent signals was made using
631 one- way ANOVA (Fig. 2C, 3C, S1B) and repeated-measures ANOVA (Fig 5A, B and 6) with
632 GraphPad Prism 8 Software (GraphPad Software, Inc., San Diego, CA, USA). Linear regressions to
633 determine the effect of cell counts (*Nmb*$^+$/PHOX2B$^+$, *Nmb*$^+$/PHOX2B$^-$, total cells) on chemoreflex
634 magnitude were run using a combined dataset for naive, NT-shRNA and PHOX2B-shRNA rats (SPSS
635 version 13.0; Fig.5C-D). p values of < 0.05 were considered significant and data are reported as
636 mean ± standard deviation (SD).

637

638

639

640 **FIGURE LEGENDS**

641 **Figure 1. Respiratory data two weeks post viral shRNA injection**. **(A)** breathing frequency (f_R,), **(B)**
642 tidal volume (V_T), **(C)** allometric minute ventilation (V_E ALLO), **(D)** oxygen consumption (VO_2 ALLO),
643 **(E)** convective requirement ratio (V_E/VO_2 ALLO), **(F)** hypercapnic ventilatory response (HCVR
644 absolute change in V_E ALLO vs. corresponding room air) of baseline (pre-surgery, grey filled box),
645 naïve (black n=8), non-target control shRNA (NT-shRNA, grey n=17) and PHOX2B shRNA (PHOX2B-
646 shRNA, red n=17) rats 2-weeks post injection during room air, hypercapnia 5% and 7.2% CO_2. f_R is
647 equally impaired in all experimental group compared to baseline but no treatment effect was
648 observed (A). V_T is significantly impaired following RTN injection in PHOX2B-shRNA group
649 compared to naïve animals ($p=0.022$) and baseline ($p< 0.001$) at 7.2% CO_2 (B). V_E ALLO is increased
650 in naïve rats compared to the other treatment groups ($p=0.005$) in room air (C). Boxplots: median,
651 1st – 3rd quartiles and 10th – 90th percentiles, outliers = dots, "+" indicates arithmetic mean.
652 Bonferroni post-hoc as indicated. Black*, different from naïve; Grey*, different from NT-shRNA;
653 Red*, different from PHOX2B sh-RNA.

654

655

656 **Figure 2. PHOX2B and *Nmb* expression and total cell count within the RTN area in naïve, NT-**
657 **shRNA and PHOX2B-shRNA injected rats two weeks post viral shRNA injection. (A)** Schematic
658 and representative image of a transverse brainstem section at the level of the RTN (-11.5 mm
659 distance from Bregma) showing the area of investigation containing RTN neurons. **(B)** Expression
660 of *Phox2b* mRNA (red), PHOX2B protein (white) and *Nmb* mRNA (green) in RTN Nmb^+/PHOX2B$^+$
661 and Nmb^+/PHOX2B$^-$ neurons in naïve (left), NT-shRNA (middle), and PHOX2B-shRNA (right) rats
662 (magnified view inserts below). Arrowheads indicate absence of PHOX2B protein. Scale

663 bar=400µm (top figures), 150µm (inserts below). **(C)** The number of total cells (*Nmb*$^{+}$/PHOX2B^{+}
664 plus *Nmb*$^{+}$/PHOX2B^{-}) comprising the RTN are reduced in PHOX2B-shRNA rats (n=4) as compared to
665 naïve (n=4) and NT-shRNA (n=4), and in NT-shRNA rats as compared to naïve rats (black$^{\#}$, One-way
666 ANOVA, p<0.001). The number of *Nmb*$^{+}$/PHOX2B^{+} cells are reduced in PHOX2B-shRNA rats as
667 compared to naïve and NT-shRNA (Blue*, One-way ANOVA, p<0 0.001). The number of
668 *Nmb*$^{+}$/PHOX2B^{-} cells was unchanged across groups. **(D,E)** Rostral-caudal distribution of
669 *Nmb*$^{+}$/PHOX2B^{+} (D) and *Nmb*$^{+}$/PHOX2B^{-} (E) neurons along the RTN.

670

671 **Figure 3. PHOX2B and *Nmb* expression and total cell count within the RTN area in naïve, NT-**
672 **shRNA and PHOX2B-shRNA injected rats 4 weeks post viral shRNA injection. (A)** Schematic and
673 representative image of a transverse brainstem section at the level of the RTN (-11.5 mm distance
674 from Bregma) showing the area of investigation containing RTN neurons. **(B)** Expression of *Phox2b*
675 mRNA (red), PHOX2B protein (white) and *Nmb* mRNA (green) in naïve (left), NT-shRNA (middle),
676 and PHOX2B-shRNA (right) rats (magnified view insert). Arrowheads indicate absence of PHOX2B
677 protein. Scale bar = 400µm (top figures), 150µm (inserts below). **(C)** The number of total cells
678 (*Nmb*$^{+}$/PHOX2B^{+} + *Nmb*$^{+}$/PHOX2B^{-}) comprising the RTN are reduced in PHOX2B-shRNA rats (n=6)
679 as compared to naïve (n=4) (Black$^{\#}$, One-way ANOVA, p=0.0087) but not to NT-shRNA (n=10). The
680 number of *Nmb*$^{+}$/PHOX2B^{+} cells are reduced in PHOX2B-shRNA rats as compared to naïve and NT-
681 shRNA (Blue*, one-way ANOVA, p<0.001). The number of *Nmb*$^{+}$/PHOX2B^{-} cells are increased in
682 PHOX2B-shRNA rats as compared to both naïve and NT-shRNA (Green*, one-way ANOVA
683 p<0.001). **(D, E)** Rostral-caudal distribution of *Nmb*$^{+}$/PHOX2B^{+} (D) and *Nmb*$^{+}$/PHOX2B^{-} (E) neurons
684 along the RTN.

685

686 **Figure 4. Respiratory data following 4 weeks post viral shRNA injection**. **(A)** breathing frequency
687 (f_R,), **(B)** tidal volume (V_T), **(C)** allometric minute ventilation (V_E ALLO), **(D)** convective requirement
688 ratio (V_E/VO_2 ALLO), **(E)** hypercapnic ventilatory response (HCVR, absolute change in V_E ALLO vs.
689 corresponding room air), **(F)** HCVR at baseline, week 2 and week 4 post-viral injections in naïve
690 (black n=8), non-target control shRNA (NT-shRNA, grey n=10) and PHOX2B-shRNA (PHOX2B-
691 shRNA, red n=6). f_R is equally impaired in all experimental group compared to baseline but no
692 treatment effect was observed (A). V_T is significantly impaired following RTN injection in PHOX2B-
693 shRNA group compared to baseline pre-surgery (p<0.001), naïve rats p<0.001), and NT-shRNA rats
694 (p=0.002) at 7.2% CO_2. (B). V_E ALLO is impaired in PHOX2B-shRNA rats during exposure to
695 hypercapnia (7.2% CO_2) compared to baseline (p=0.0025), naïve rats (p=0.007), and NT-shRNA rats
696 (p=0.002). (C). V_E/VO_2 ALLO is reduced in PHOX2B-shRNA animals compared to NT-shRNA rats
697 both at 5% (p=0.023) and 7.2% (p=0.004.) CO_2 (D). HCVR during 7.2% CO_2 is lower in PHOX2B-
698 shRNA rats compared to baseline (p=0.007), naïve rats (p=0.001), and NT-shRNA rats (p=0.016) (E).
699 Boxplots: median, 1st – 3rd quartiles and 10th – 90th percentiles, outliers = dots, "+" indicates
700 arithmetic mean. Bonferroni post-hoc as indicated. HCVR is significantly impaired only in PHOX2B-
701 shRNA rats 4-weeks post-surgery (One-way ANOVA p=0.007) (F). Black*, different from naïve;
702 Grey*, different from NT-shRNA; Red*, different from PHOX2B- shRNA.

703

704 **Figure 5. PHOX2B knockdown in RTN neurons does not alter TH or *Nmb* expression but impairs**
705 **the hypercapnic ventilatory response. (A)** No differences are observed in the rostral-caudal
706 distribution of $TH^+/PHOX2B^+$ catecholaminergic C1 neurons cells caudal to the RTN between naïve
707 (black, n=4), NT-shRNA (grey, n=10) and PHOX2B-shRNA (red, n=6) rats. **(B)** Quantification of *Nmb*
708 mRNA fluorescence staining intensity along the rostro-caudal extension of RTN in naïve (black,
709 n=4), NT-shRNA (grey, n=10) and PHOX2B-shRNA (red, n=6) rat calculated as ratio RTN/NTS shows

710 no difference between treatment groups. **(D-E)** X-Y plot of HCVR during 7.2% CO_2 exposure
711 relative to the number of *Nmb*$^+$/PHOX2B$^+$ (D, slope is different from "0" at $p<0.001$; $r^2=0.739$) and
712 *Nmb*$^+$/PHOX2B$^-$ (E, $p<0.001$ for difference between slopes; $r^2=0.482$) in the RTN.

713

714 **Figure 6. Gpr4 and Task2 mRNA expression within the RTN area in naïve, and PHOX2B-shRNA**
715 **injected rats 4 weeks post viral shRNA injection. (A,D)** *Nmb* (green), *Gpr4*, *Task2* mRNA (red) and
716 PHOX2B protein (grey) expression in RTN neurons in naïve (top) and PHOX2B-shRNA (bottom) rats.
717 Scale bar = 150 µm. Arrowheads indicate colocalization of *Gpr4* (A) and *Task2* (D) with
718 *Nmb*$^+$/PHOX2B$^+$ neurons. Asterisks indicate colocalization of *Gpr4* (A) and *Task2* (D) with
719 *Nmb*$^+$/PHOX2B$^-$ neurons. **(B,E)** Quantification of *Gpr4* and *Task2* mRNA fluorescence staining
720 intensity along the rostro-caudal extension of RTN in naïve (black), NT-shRNA (grey) and PHOX2B-
721 shRNA (red) rats. Black*, different from naïve, Grey*, different from NT-shRNA (**C and F**)
722 Quantification of *Gpr4* and *Task2* mRNA fluorescence staining intensity along the rostro-caudal
723 extension of RTN in Nmb$^+$/PHOX2B$^+$ (red filled dot) and Nmb$^+$/PHOX2B$^-$ (red empty dot) neurons in
724 PHOX2B-shRNA rats. Mean corrected total cell fluorescence (CTCF) value ± SEM combined (naïve,
725 n=4; NT-shRNA, n=10; PHOX2B-shRNA, n=6) (see methods for detail). One-way ANOVA repeated
726 measures.

727

728 **Supplementary Fig. 1. (A)** Allometric V_E is equally impaired following RTN injection of non-target
729 control (NT-shRNA n=6) and PHOX2B-shRNA (n=8). Asterisks, difference from baseline. **(B)** The
730 number of Nmb$^+$/PHOX2B$^+$ cells comprising the RTN are reduced in NT-shRNA (n=5), and shRNA
731 rats (n=5) as compared to naive controls (n=4; Asterisks, difference from baseline). The number of
732 Nmb$^+$/PHOX2B$^-$ cells was unchanged in both surgical treatments compared to baseline.

733 **REFERENCES**

734 Abbott, S. B. G., Stornetta, R. L., Coates, M. B., & Guyenet, P. G. (2011). *Phox2b-Expressing*
735 *Neurons of the Parafacial Region Regulate Breathing Rate, Inspiration, and Expiration in*
736 *Conscious Rats*. https://doi.org/10.1523/JNEUROSCI.3280-11.2011

737 Amiel, J., Laudier, B., Attié-Bitach, T., Trang, H., De Pontual, L., Gener, B., Trochet, D., Etchevers, H.,
738 Ray, P., Simonneau, M., Vekemans, M., Munnich, A., Gaultier, C., & Lyonnet, S. (2003).
739 Polyalanine expansion and frameshift mutations of the paired-like homeobox gene PHOX2B in
740 congenital central hypoventilation syndrome. *Nature Genetics*, *33*(4), 459–461.
741 https://doi.org/10.1038/ng1130

742 Bachetti, T., Matera, I., Borghini, S., Duca, M. Di, Ravazzolo, R., & Ceccherini, I. (2005). Distinct
743 pathogenetic mechanisms for PHOX2B associated polyalanine expansions and frameshift
744 mutations in congenital central hypoventilation syndrome. *Human Molecular Genetics*, *14*(13),
745 1815–1824. https://doi.org/10.1093/hmg/ddi188

746 Barna, B. F., Takakura, A. C., Mulkey, D. K., & Moreira, T. S. (2016). Purinergic receptor blockade in
747 the retrotrapezoid nucleus attenuates the respiratory chemoreflexes in awake rats. *Acta*
748 *Physiologica (Oxford, England)*, *217*(1), 80–93. https://doi.org/10.1111/APHA.12637

749 Basting, T. M., Burke, P. G. R., Kanbar, R., Viar, K. E., Stornetta, D. S., Stornetta, R. L., & Guyenet, P.
750 G. (2015). *Hypoxia Silences Retrotrapezoid Nucleus Respiratory Chemoreceptors via Alkalosis*.
751 https://doi.org/10.1523/JNEUROSCI.2923-14.2015

752 Berry-Kravis, E. M., Zhou, L., Rand, C. M., & Weese-Mayer, D. E. (2006). Congenital central
753 hypoventilation syndrome PHOX2B mutations and phenotype. *American Journal of Respiratory*
754 *and Critical Care Medicine*, *174*(10), 1139–1144. https://doi.org/10.1164/rccm.200602-305OC

755 Biancardi, V., Saini, J., Pageni, A., Prashaad M., H., Funk, G. D., & Pagliardini, S. (2021). Mapping of
756 the excitatory, inhibitory, and modulatory afferent projections to the anatomically defined
757 active expiratory oscillator in adult male rats. *Journal of Comparative Neurology*, *529*(4), 853–
758 884. https://doi.org/10.1002/CNE.24984

759 Bourdeaut, F., Trochet, D., Janoueix-Lerosey, I., Ribeiro, A., Deville, A., Coz, C., Michiels, J. F.,
760 Lyonnet, S., Amiel, J., & Delattre, O. (2005). Germline mutations of the paired-like homeobox 2B
761 (PHOX2B) gene in neuroblastoma. In *Cancer Letters* (Vol. 228, Issues 1–2, pp. 51–58). Elsevier.
762 https://doi.org/10.1016/j.canlet.2005.01.055

763 Brunet, J. F., & Pattyn, A. (2002). Phox2 genes - From patterning to connectivity. In *Current Opinion*
764 *in Genetics and Development* (Vol. 12, Issue 4, pp. 435–440). https://doi.org/10.1016/S0959-
765 437X(02)00322-2

766 Cardani, S., Janes, T. A., Saini, J. K., Di Lascio, S., Benfante, R., Fornasari, D., & Pagliardini, S. (2022).
767 Etonogestrel Administration Reduces the Expression of PHOX2B and Its Target Genes in the
768 Solitary Tract Nucleus. *International Journal of Molecular Sciences*, *23*(9).
769 https://doi.org/10.3390/ijms23094816

770 Cutsforth-Gregory, J. K., & Benarroch, E. E. (2017). Nucleus of the solitary tract, medullary reflexes,
771 and clinical implications. *Neurology*, *88*(12), 1187–1196.
772 https://doi.org/10.1212/WNL.0000000000003751

773 Dauger, S. (2003). Phox2b controls the development of peripheral chemoreceptors and afferent
774 visceral pathways. *Development*, *130*(26), 6635–6642. https://doi.org/10.1242/dev.00866

775 Depocas, F., & Sanford Hart, J. (n.d.). *Use of the Pdzlling Oxygen Analyzer for Memwement of*
776 *Oxygen conszlm~tion of Ahmds iti Open-Circuit Systems ad in a Short-Lag, Closed-Cirwit Appma*
777 *tml*.

778 Di Lascio, S., Bachetti, T., Saba, E., Ceccherini, I., Benfante, R., & Fornasari, D. (2013).
779 Transcriptional dysregulation and impairment of PHOX2B auto-regulatory mechanism induced
780 by polyalanine expansion mutations associated with congenital central hypoventilation
781 syndrome. *Neurobiology of Disease*, *50*(1), 187–200. https://doi.org/10.1016/j.nbd.2012.10.019

782 Di Lascio, S., Belperio, D., Benfante, R., & Fornasari, D. (2016). Alanine expansions associated with
783 congenital central hypoventilation syndrome impair PHOX2B homeodomain-mediated
784 dimerization and nuclear import. *Journal of Biological Chemistry*, *291*(25), 13375–13393.
785 https://doi.org/10.1074/jbc.M115.679027

786 Di Lascio, S., Benfante, R., Cardani, S., & Fornasari, D. (2018). Advances in the molecular biology
787 and pathogenesis of congenital central hypoventilation syndrome—implications for new
788 therapeutic targets. *Expert Opinion on Orphan Drugs*, *00*(00), 1–13.
789 https://doi.org/10.1080/21678707.2018.1540978

790 Di Lascio, S., Benfante, R., Cardani, S., & Fornasari, D. (2021). Research Advances on Therapeutic
791 Approaches to Congenital Central Hypoventilation Syndrome (CCHS). *Frontiers in Neuroscience*,
792 *14*. https://doi.org/10.3389/FNINS.2020.615666

793 Di Lascio, S., Benfante, R., Zanni, E. Di, Cardani, S., Adamo, A., Fornasari, D., Ceccherini, I., &
794 Bachetti, T. (2018). *Structural and functional differences in PHOX2B frameshift mutations*
795 *underlie isolated or syndromic congenital central hypoventilation syndrome*.
796 https://doi.org/10.1002/humu.23365

797 Drorbaugh, J. E., & Fenn, W. O. (1955). A barometric method for measuring ventilation in newborn
798 infants. *Pediatrics*, *16*(1), 81–87. https://doi.org/10.1542/peds.16.1.81

799 Dubreuil, V., Ramanantsoa, N., Trochet, D., Vaubourg, V., Amiel, J., Gallego, J., Brunet, J.-F., &
800 Goridis, C. (2008). A human mutation in Phox2b causes lack of CO2 chemosensitivity, fatal
801 central apnea, and specific loss of parafacial neurons. *Proceedings of the National Academy of*
802 *Sciences*, *105*(3), 1067–1072. https://doi.org/10.1073/pnas.0709115105

803 Dubreuil, V., Thoby-Brisson, M., Rallu, M., Persson, K., Pattyn, A., Birchmeier, C., Brunet, J.-F.,
804 Fortin, G., & Goridis, C. (2009). Defective Respiratory Rhythmogenesis and Loss of Central
805 Chemosensitivity in Phox2b Mutants Targeting Retrotrapezoid Nucleus Neurons. *Journal of*
806 *Neuroscience*, *29*(47), 14836–14846. https://doi.org/10.1523/JNEUROSCI.2623-09.2009

807 Durand, E., Dauger, S., Pattyn, A., Gaultier, C., Goridis, C., & Gallego, J. (2005). Sleep-disordered
808 breathing in newborn mice heterozygous for the transcription factor phox2b. *American Journal*

809 *of Respiratory and Critical Care Medicine*, *172*(2), 238–243.
810 https://doi.org/10.1164/rccm.200411-1528OC

811 Fan, Y., Huang, J., Duffourc, M., Kao, R. L., Ordway, G. A., Huang, R., & Zhu, M. Y. (2011).
812 Transcription factor Phox2 upregulates expression of norepinephrine transporter and
813 dopamine β-hydroxylase in adult rat brains. *Neuroscience*, *192*, 37–53.
814 https://doi.org/10.1016/j.neuroscience.2011.07.005

815 Gestreau, C., Heitzmann, D., Thomas, J., Dubreuil, V., Bandulik, S., Reichold, M., Bendahhou, S.,
816 Pierson, P., Sterner, C., Peyronnet-Roux, J., Benfriha, C., Tegtmeier, I., Ehnes, H., Georgieff, M.,
817 Lesage, F., Brunet, J.-F., Goridis, C., Warth, R., & Barhanin, J. (2010). Task2 potassium channels
818 set central respiratory CO2 and O2 sensitivity. *Proceedings of the National Academy of Sciences*,
819 *107*(5), 2325–2330. https://doi.org/10.1073/pnas.0910059107

820 Goridis, C., Dubreuil, V., Thoby-brisson, M., & Fortin, G. (2010). *Seminars in Cell & Developmental*
821 *Biology Phox2b , congenital central hypoventilation syndrome and the control of respiration*. *21*,
822 814–822. https://doi.org/10.1016/j.semcdb.2010.07.006

823 Gourine, A. V, Llaudet, E., Dale, N., & Spyer, K. M. (2005). *Behavioral/Systems/Cognitive Release of*
824 *ATP in the Ventral Medulla during Hypoxia in Rats: Role in Hypoxic Ventilatory Response*.
825 https://doi.org/10.1523/JNEUROSCI.3763-04.2005

826 Guyenet, P. G., Bayliss, D. A., Stornetta, R. L., Ludwig, M. G., Kumar, N. N., Shi, Y., Burke, P. G. R.,
827 Kanbar, R., Basting, T. M., Holloway, B. B., & Wenker, I. C. (2016). Proton detection and
828 breathing regulation by the retrotrapezoid nucleus. *Journal of Physiology*, *594*(6), 1529–1551.
829 https://doi.org/10.1113/JP271480

830 Guyenet, P. G., Stornetta, R. L., Souza, G. M. P. R., Abbott, S. B. G., Shi, Y., & Bayliss, D. A. (2019).
831 The Retrotrapezoid Nucleus: Central Chemoreceptor and Regulator of Breathing Automaticity.
832 *Trends in Neurosciences*, *42*(11), 807–824. https://doi.org/10.1016/J.TINS.2019.09.002

833 Harper, R. M., Kumar, R., Macey, P. M., Harper, R. K., & Ogren, J. A. (2015). Impaired neural
834 structure and function contributing to autonomic symptoms in congenital central
835 hypoventilation syndrome. *Frontiers in Neuroscience*, *9*(OCT), 415.
836 https://doi.org/10.3389/FNINS.2015.00415

837 Janes, T. A., Cardani, S., Saini, J. K., & Pagliardini, S. (2024). *Title: Etonogestrel promotes respiratory*
838 *recovery in an in vivo rat model of central chemoreflex impairment. Running title: Chemoreflex*
839 *recovery by etonogesterel*.

840 Kang, B. J., Chang, D. A., Mackay, D. D., West, G. H., Moreira, T. S., Takakura, A. C., Gwilt, J. M.,
841 Guyenet, P. G., & Stornetta, R. L. (2007). Central nervous system distribution of the
842 transcription factor Phox2b in the adult rat. *Journal of Comparative Neurology*, *503*(5), 627–
843 641. https://doi.org/10.1002/cne.21409

844 Kumar, N. N., Velic, A., Soliz, J., Shi, Y., Li, K., Wang, S., Weaver, J. L., Sen, J., Abbott, S. B. G.,
845 Lazarenko, R. M., Ludwig, M. G., Perez-Reyes, E., Mohebbi, N., Bettoni, C., Gassmann, M., Suply,
846 T., Seuwen, K., Guyenet, P. G., Wagner, C. A., & Bayliss, D. A. (2015). Regulation of breathing by
847 CO2 requires the proton-activated receptor GPR4 in retrotrapezoid nucleus neurons. *Science*,
848 *348*(6240), 1255–1260. https://doi.org/10.1126/science.aaa0922

849 Lighton, J. R. B. (2021). *MEASURING METABOLIC RATES : a manual for scientists.*
850 https://global.oup.com/academic/product/measuring-metabolic-rates-9780198869320

851 Madani, A., Pitollat, G., Sizun, E., Cardoit, L., Ringot, M., Bourgeois, T., Ramanantsoa, N., Delclaux,
852 C., Dauger, S., Thoby-Brisson, M., Gallego, J., & Matrot, B. (2021). Obstructive Apneas in a
853 Mouse Model of Congenital Central Hypoventilation Syndrome. American journal of respiratory
854 and critical care medicine, 204(10), 1200–1210. https://doi.org/10.1164/rccm.202104-0887OC.

855 Marina, N., Abdala, A. P., Trapp, S., Li, A., Nattie, E. E., Hewinson, J., Smith, J. C., Paton, J. F. R., &
856 Gourine, A. V. (2010). Essential Role of Phox2b-Expressing Ventrolateral Brainstem Neurons in
857 the Chemosensory Control of Inspiration and Expiration. *Journal of Neuroscience*, *30*(37),
858 12466–12473. https://doi.org/10.1523/JNEUROSCI.3141-10.2010

859 Matera, I. (2004). PHOX2B mutations and polyalanine expansions correlate with the severity of the
860 respiratory phenotype and associated symptoms in both congenital and late onset Central
861 Hypoventilation syndrome. *Journal of Medical Genetics*, *41*(5), 373–380.
862 https://doi.org/10.1136/jmg.2003.015412

863 Mcbride, J. L., Boudreau, R. L., Harper, S. Q., Staber, P. D., Monteys, A. M., Martins, I. S., Gilmore,
864 B. L., Burstein, H., Peluso, R. W., Polisky, B., Carter, B. J., & Davidson, B. L. (2008). Artificial
865 miRNAs mitigate shRNA-mediated toxicity in the brain: implications for the therapeutic
866 development of RNAi. Proceedings of the National Academy of Sciences of the United States of
867 America, 105(15), 5868–5873. https://doi.org/10.1073/pnas.0801775105

868 McCloy, R. A., Rogers, S., Caldon, C. E., Lorca, T., Castro, A., & Burgess, A. (2014). Partial inhibition
869 of Cdk1 in G2 phase overrides the SAC and decouples mitotic events. *Cell Cycle*, *13*(9), 1400–
870 1412. https://doi.org/10.4161/CC.28401/SUPPL_FILE/KCCY_A_10928401_SM0001.ZIP

871 Mortola, J. P., & Frappell, P. B. (1998). On the barometric method for measurements of
872 ventilation, and its use in small animals.

873 Mortola, J. P., Matsuoka, T., Saiki, C., & Naso, L. (1994). RESPIRATION PHYSIOLOGY Metabolism
874 and ventilation in hypoxic rats: effect of body mass. *Respiration Physiology*, *97*, 225–234.

875 Nagashimada, M., Ohta, H., Li, C., Nakao, K., Uesaka, T., Brunet, J. F., Amiel, J., Trochet, D.,
876 Wakayama, T., & Enomoto, H. (2012). Autonomic neurocristopathy-associated mutations in
877 PHOX2B dysregulate Sox10 expression. *Journal of Clinical Investigation*, *122*(9), 3145–3158.
878 https://doi.org/10.1172/JCI63401

879 Nattie, E. E., & Li, A. (1994). Retrotrapezoid nucleus lesions decrease phrenic activity and CO2
880 sensitivity in rats. *Respiration Physiology*, *97*(1), 63–77. https://doi.org/10.1016/0034-
881 5687(94)90012-4

882 Nattie, E. E., & Li, A. (2002). Substance P-saporin lesion of neurons with NK1 receptors in one
883 chemoreceptor site in rats decreases ventilation and chemosensitivity. *The Journal of*
884 *Physiology*, *544*(2), 603–616. https://doi.org/10.1113/JPHYSIOL.2002.020032

885 Nobuta, H., Cilio, M. R., Danhaive, O., Tsai, H.-H., Tupal, S., Chang, S. M., Murnen, A., Kreitzer, F.,
886 Bravo, V., Czeisler, C., Gokozan, H. N., Gygli, P., Bush, S., Weese-Mayer, D. E., Conklin, B., Yee,
887 S.-P., Huang, E. J., Gray, P. A., Rowitch, D., & Otero, J. J. (2015). Dysregulation of locus coeruleus

development in congenital central hypoventilation syndrome. *Acta Neuropathologica*, *130*(2), 171–183. https://doi.org/10.1007/s00401-015-1441-0

Parodi, S., Di Zanni, E., Di Lascio, S., Bocca, P., Prigione, I., Fornasari, D., Pennuto, M., Bachetti, T., Ceccherini, I., Zanni, E. Di, Lascio, D., Bocca, P., Prigione, I., Fornasari, D., Pennuto, M., & Bachetti, T. (2012). The E3 ubiquitin ligase TRIM11 mediates the degradation of congenital central hypoventilation syndrome-associated polyalanine-expanded PHOX2B. *Journal of Molecular Medicine*, *90*(9), 1025–1035. https://doi.org/10.1007/s00109-012-0868-1

Pattyn, A., Hirsch, M. R., Goridis, C., & Brunet, J. F. (2000). Control of hindbrain motor neuron differentiation by the homeobox gene Phox2b. *Development (Cambridge, England)*, *127*(7), 1349–1358. https://doi.org/10.1242/DEV.127.7.1349

Pattyn, A., Morin, X., & Cremer, H. (1999). *The homeobox gene Phox2b is essential for the development of autonomic neural crest derivatives*. *399*(May).

Pattyn, A., Morin, X., Cremer, H., Goridis, C., & Brunet, J. F. (1997). Expression and interactions of the two closely related homeobox genes Phox2a and Phox2b during neurogenesis. *Development (Cambridge, England)*, *124*(20), 4065–4075. http://www.ncbi.nlm.nih.gov/pubmed/9374403

Paxinos, G., & Watson, C. *The rat brain in stereotaxic coordinates*.

Pirone, L., Caldinelli, L., Di Lascio, S., Di Girolamo, R., Di Gaetano, S., Fornasari, D., Pollegioni, L., Benfante, R., & Pedone, E. (2019). Molecular insights into the role of the polyalanine region in mediating PHOX2B aggregation. *FEBS Journal*, *286*(13), 2505–2521. https://doi.org/10.1111/FEBS.14841

Ramanantsoa, N., Hirsch, M.-R., Thoby-Brisson, M., Dubreuil, V., Bouvier, J., Ruffault, P.-L., Matrot, B., Fortin, G., Brunet, J.-F., Gallego, J., & Goridis, C. (2011). Breathing without CO2 Chemosensitivity in Conditional Phox2b Mutants. *Journal of Neuroscience*, *31*(36), 12880–12888. https://doi.org/10.1523/JNEUROSCI.1721-11.2011

Seifert, E. L., Knowles, J., & Mortola, J. P. (2000). Continuous circadian measurements of ventilation in behaving adult rats. *Respiration Physiology*, *120*, 179–183. www.elsevier.com/locate/resphysiol

Shi, Y., Stornetta, R. L., Stornetta, D. S., Suna Onengut-Gumuscu, X., Farber, E. A., Turner, S. D., Guyenet, P. G., & Bayliss, D. A. (2017). *Neuromedin B Expression Defines the Mouse Retrotrapezoid Nucleus*. https://doi.org/10.1523/JNEUROSCI.2055-17.2017

Shimokaze, T., Sasaki, A., Meguro, T., Hasegawa, H., Hiraku, Y., Yoshikawa, T., Kishikawa, Y., & Hayasaka, K. (2015). Genotype-phenotype relationship in Japanese patients with congenital central hypoventilation syndrome. *Journal of Human Genetics*, *60*(9), 473–477. https://doi.org/10.1038/jhg.2015.65

Souza, G. M. P. R., Kanbar, R., Stornetta, D. S., Abbott, S. B. G., Stornetta, R. L., & Guyenet, P. G. (2018). Breathing regulation and blood gas homeostasis after near complete lesions of the retrotrapezoid nucleus in adult rats. *Journal of Physiology*, *596*(13), 2521–2545. https://doi.org/10.1113/JP275866

927 Souza, G. M. P. R., Stornetta, D. S., Shi, Y., Lim, E., Berry, F. E., Bayliss, D. A., & Abbott, S. B. G.
928 (2023). Neuromedin B-Expressing Neurons in the Retrotrapezoid Nucleus Regulate Respiratory
929 Homeostasis and Promote Stable Breathing in Adult Mice. *Journal of Neuroscience*, *43*(30),
930 5501–5520. https://doi.org/10.1523/JNEUROSCI.0386-23.2023

931 Stanke, M., Junghans, D., Geissen, M., Goridis, C., Ernsberger, U., & Rohrer, H. (1999). The Phox2
932 homeodomain proteins are sufficient to promote the development of sympathetic neurons.
933 *Development*, *126*(18), 4087–4094. https://doi.org/10.1242/dev.00165

934 Stornetta, R. L., Moreira, T. S., Takakura, A. C., Kang, B. J., Chang, D. A., West, G. H., Mulkey, D. K.,
935 Bayliss, D. A., & Guyenet, P. G. (2006). *Expression of Phox2b by Brainstem Neurons Involved in*
936 *Chemosensory Integration in the Adult Rat*. *26*(40), 10305–10314.
937 https://doi.org/10.1523/JNEUROSCI.2917-06.2006

938 Takakura, A. C., Barna, B. F., Cruz, J. C., Colombari, E., & Moreira, T. S. (2014). Phox2b-expressing
939 retrotrapezoid neurons and the integration of central and peripheral chemosensory control of
940 breathing in conscious rats. *Experimental Physiology*, *99*(3).
941 https://doi.org/10.1113/expphysiol.2013.076752

942 Takakura, A. C., Moreira, T. S., Stornetta, R. L., West, G. H., Gwilt, J. M., & Guyenet, P. G. (2008).
943 Selective lesion of retrotrapezoid Phox2b-expressing neurons raises the apnoeic threshold in
944 rats. *The Journal of Physiology*, *586*(Pt 12), 2975.
945 https://doi.org/10.1113/JPHYSIOL.2008.153163

946 Tiveron, M. C., Hirsch, M. R., & Brunet, J. F. (1996). The expression pattern of the transcription
947 factor Phox2 delineates synaptic pathways of the autonomic nervous system. *The Journal of*
948 *Neuroscience : The Official Journal of the Society for Neuroscience*, *16*(23), 7649–7660.
949 https://doi.org/10.1523/JNEUROSCI.16-23-07649.1996

950 Trang, H., Dehan, M., Beaufils, F., Zaccaria, I., Amiel, J., & Gaultier, C. (2005). The French
951 Congenital Central Hypoventilation Syndrome Registry. *Chest*, *127*(1), 72–79.
952 https://doi.org/10.1378/chest.127.1.72

953 Trochet, D., de Pontual, L., Estêvao, M. H., Mathieu, Y., Munnich, A., Feingold, J., Goridis, C.,
954 Lyonnet, S., & Amiel, J. (2008). Homozygous mutation of the PHOX2B gene in congenital central
955 hypoventilation syndrome (Ondine's Curse). *Human Mutation*, *29*(5), 770–770.
956 https://doi.org/10.1002/humu.20727

957 Trochet, D., Hong, S. J., Lim, J. K., Brunet, J. F., Munnich, A., Kim, K. S., Lyonnet, S., Goridis, C., &
958 Amiel, J. (2005). Molecular consequences of PHOX2B missense, frameshift and alanine
959 expansion mutations leading to autonomic dysfunction. *Human Molecular Genetics*, *14*(23),
960 3697–3708. https://doi.org/10.1093/hmg/ddi401

961 Van Gestel, M. A., Van Erp, S., Sanders, L. E., Brans, M. A. D., Luijendijk, M. C. M., Merkestein, M.,
962 Pasterkamp, R. J., & Adan, R. A. H. (2014). shRNA-induced saturation of the microRNA pathway
963 in the rat brain. *Gene Therapy*, *21*(2), 205–211. https://doi.org/10.1038/GT.2013.76

964 Van Limpt, V., Schramm, A., Lakeman, A., Van Sluis, P., Chan, A., Van Noesel, M., Baas, F., Caron,
965 H., Eggert, A., & Versteeg, R. (2004). The Phox2B homeobox gene is mutated in sporadic
966 neuroblastomas. *Oncogene*, *23*(57), 9280–9288. https://doi.org/10.1038/sj.onc.1208157

967 Weese-Mayer, D. E., Berry-Kravis, E. M., Zhou, L., Maher, B. S., Silvestri, J. M., Curran, M. E., &
968 Marazita, M. L. (2003). Idiopathic congenital central hypoventilation syndrome: Analysis of
969 genes pertinent to early autonomic nervous system embryologic development and
970 identification of mutations in PHOX2b. *American Journal of Medical Genetics*, *123A*(3), 267–
971 278. https://doi.org/10.1002/ajmg.a.20527

972 Weese-Mayer, D. E., Rand, C. M., Zhou, A., Carroll, M. S., & Hunt, C. E. (2017). Congenital central
973 hypoventilation syndrome: A bedside-to-bench success story for advancing early diagnosis and
974 treatment and improved survival and quality of life. In *Pediatric Research* (Vol. 81, Issues 1–2).
975 https://doi.org/10.1038/pr.2016.196

976 Wickström, H. R., Berner, J., Holgert, H., Hökfelt, T., & Lagercrantz, H. (2004). Hypoxic response in
977 newborn rat is attenuated by neurokinin-1 receptor blockade. *Respiratory Physiology and*
978 *Neurobiology*, *140*(1), 19–31. https://doi.org/10.1016/j.resp.2004.01.008

979 Wu, H., Su, Y., Hung, C., Hsieh, W., & Wu, K. (2009). *Interaction Between PHOX2B and CREBBP*
980 *Mediates Synergistic Activation : Mechanistic Implications of PHOX2B Mutants Human*
981 *Mutation*. https://doi.org/10.1002/humu.20929

982 Zoccal, D. B., Furuya, W. I., Bassi, M., A Colombari, D. S., Colombari, E., Hildreth, C., & Putnam, R.
983 W. (2014). *The nucleus of the solitary tract and the coordination of respiratory and sympathetic*
984 *activities*. https://doi.org/10.3389/fphys.2014.00238

985

986

987

988

989

990

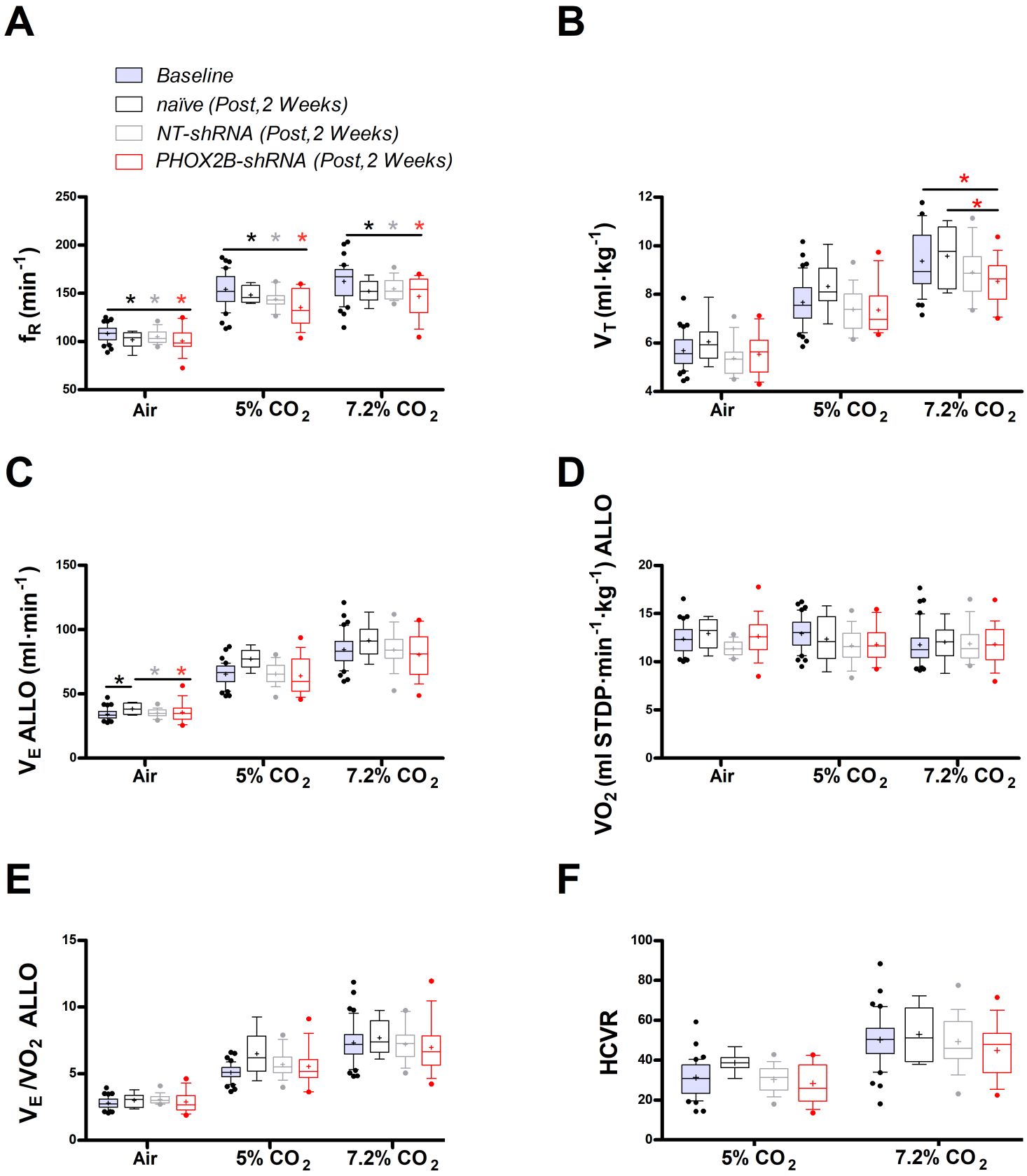
A
Baseline
naïve (Post,2 Weeks)
NT-shRNA (Post,2 Weeks)
PHOX2B-shRNA (Post,2 Weeks)
f_R (min^{-1})
250
200
150
100
50
Air
5% CO_2
7.2% CO_2
B
V_T (ml·kg^{-1})
12
10
8
6
4
Air
5% CO_2
7.2% CO_2
C
V_E ALLO (ml·min^{-1})
150
100
50
0
Air
5% CO_2
7.2% CO_2
D
VO_2 (ml STDP·min^{-1}·kg^{-1}) ALLO
20
15
10
5
0
Air
5% CO_2
7.2% CO_2
E
V_E /VO_2 ALLO
15
10
5
0
Air
5% CO_2
7.2% CO_2
F
HCVR
100
80
60
40
20
0
5% CO_2
7.2% CO_2

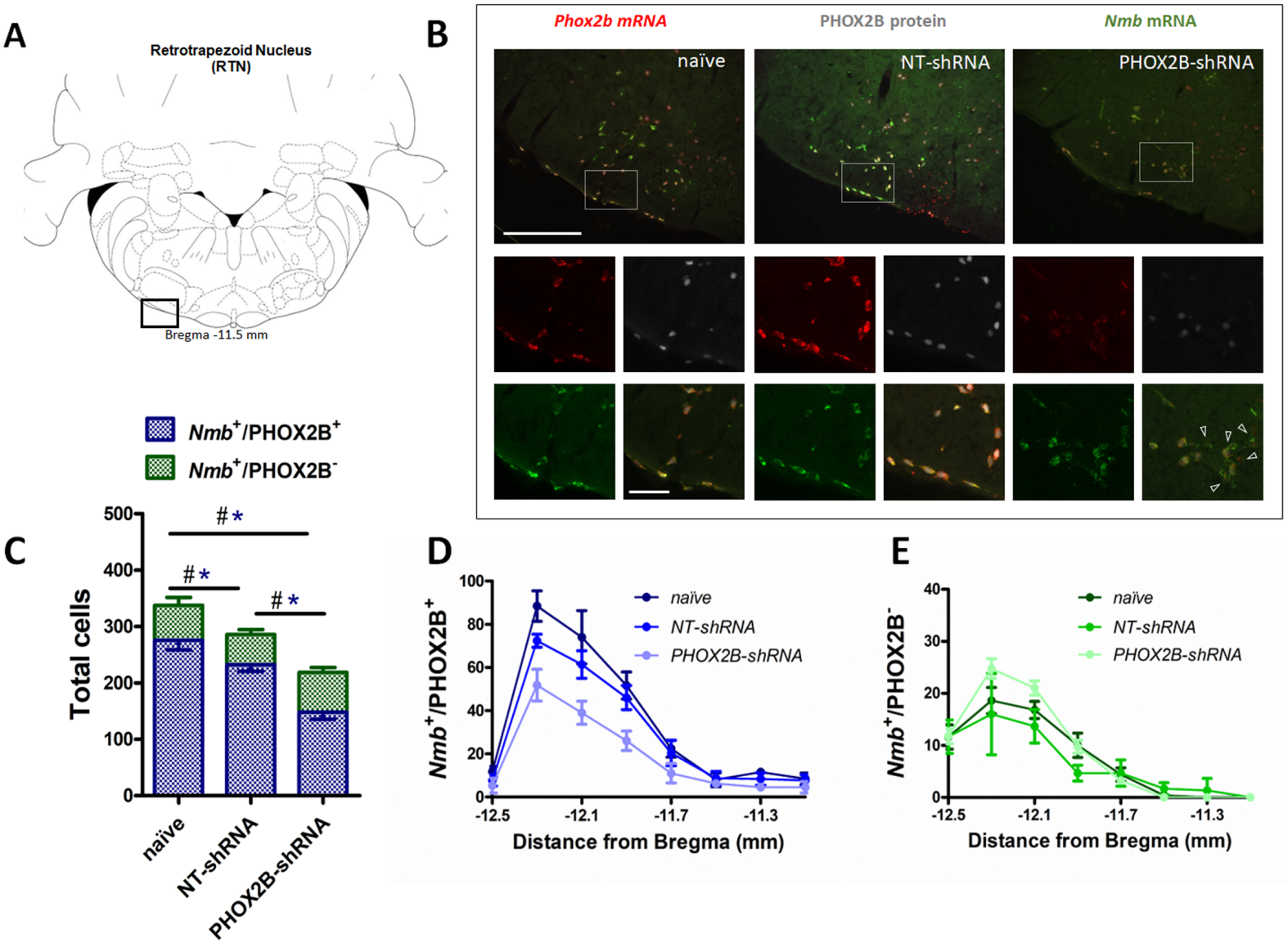
A
Retrotrapezoid Nucleus
(RTN)
Bregma -11.5 mm
B
Phox2b mRNA
PHOX2B protein
Nmb mRNA
naïve
NT-shRNA
PHOX2B-shRNA
Nmb+/PHOX2B+
Nmb+/PHOX2B-
C
Total cells
500
400
300
200
100
0
#*
#*
#*
naïve
NT-shRNA
PHOX2B-shRNA
D
Nmb+/PHOX2B+
100
80
60
40
20
0
naïve
NT-shRNA
PHOX2B-shRNA
-12.5
-12.1
-11.7
-11.3
Distance from Bregma (mm)
E
Nmb+/PHOX2B-
40
30
20
10
0
naïve
NT-shRNA
PHOX2B-shRNA
-12.5
-12.1
-11.7
-11.3
Distance from Bregma (mm)

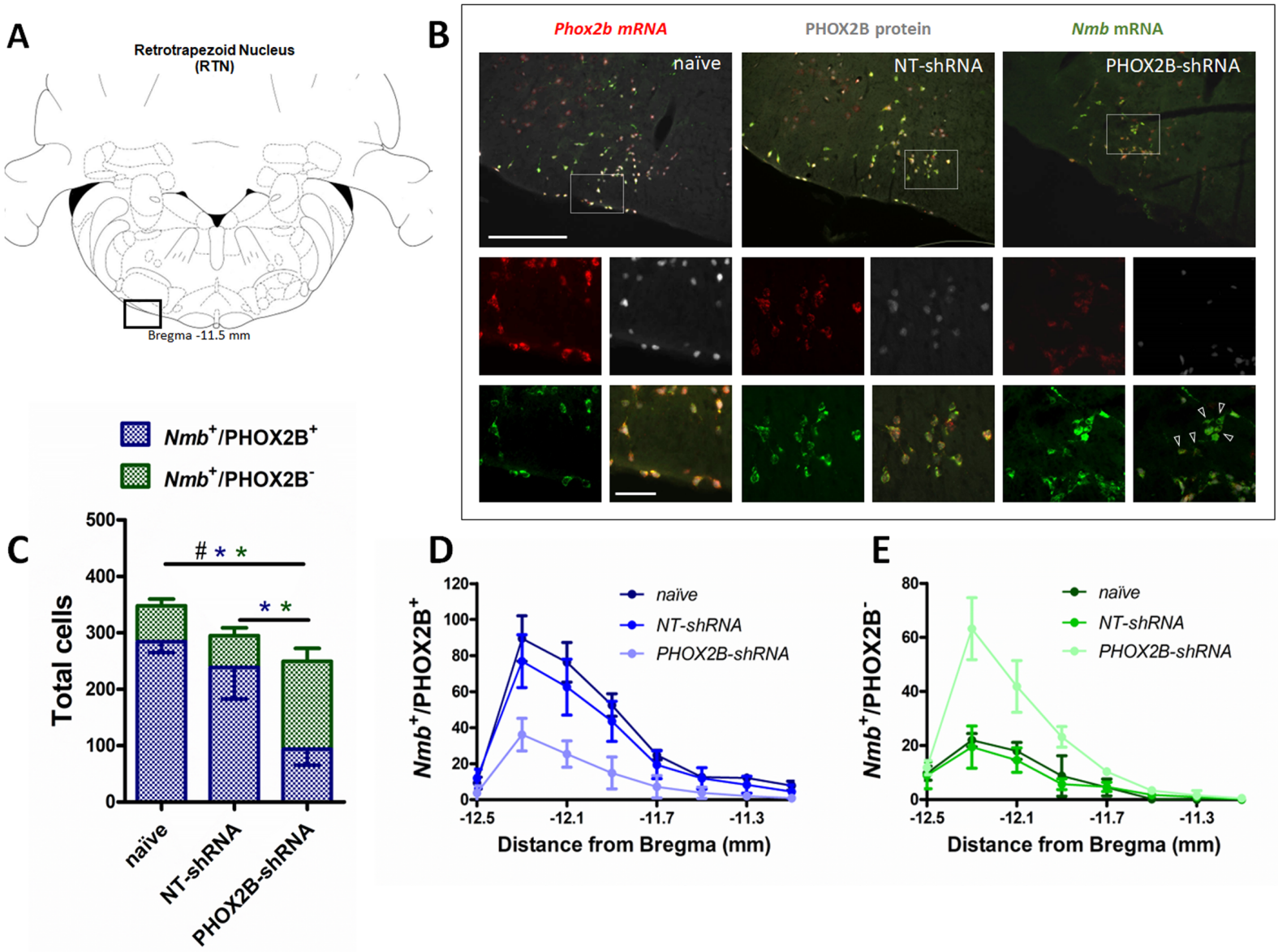
A
Retrotrapezoid Nucleus
(RTN)
Bregma -11.5 mm
B
Phox2b mRNA
PHOX2B protein
Nmb mRNA
naïve
NT-shRNA
PHOX2B-shRNA
C
Nmb+/PHOX2B+
Nmb+/PHOX2B-
Total cells
500
400
300
200
100
0
* *
* *
naïve
NT-shRNA
PHOX2B-shRNA
D
Nmb+/PHOX2B+
120
100
80
60
40
20
0
naïve
NT-shRNA
PHOX2B-shRNA
-12.5
-12.1
-11.7
-11.3
Distance from Bregma (mm)
E
Nmb+/PHOX2B-
80
60
40
20
0
naïve
NT-shRNA
PHOX2B-shRNA
-12.5
-12.1
-11.7
-11.3
Distance from Bregma (mm)

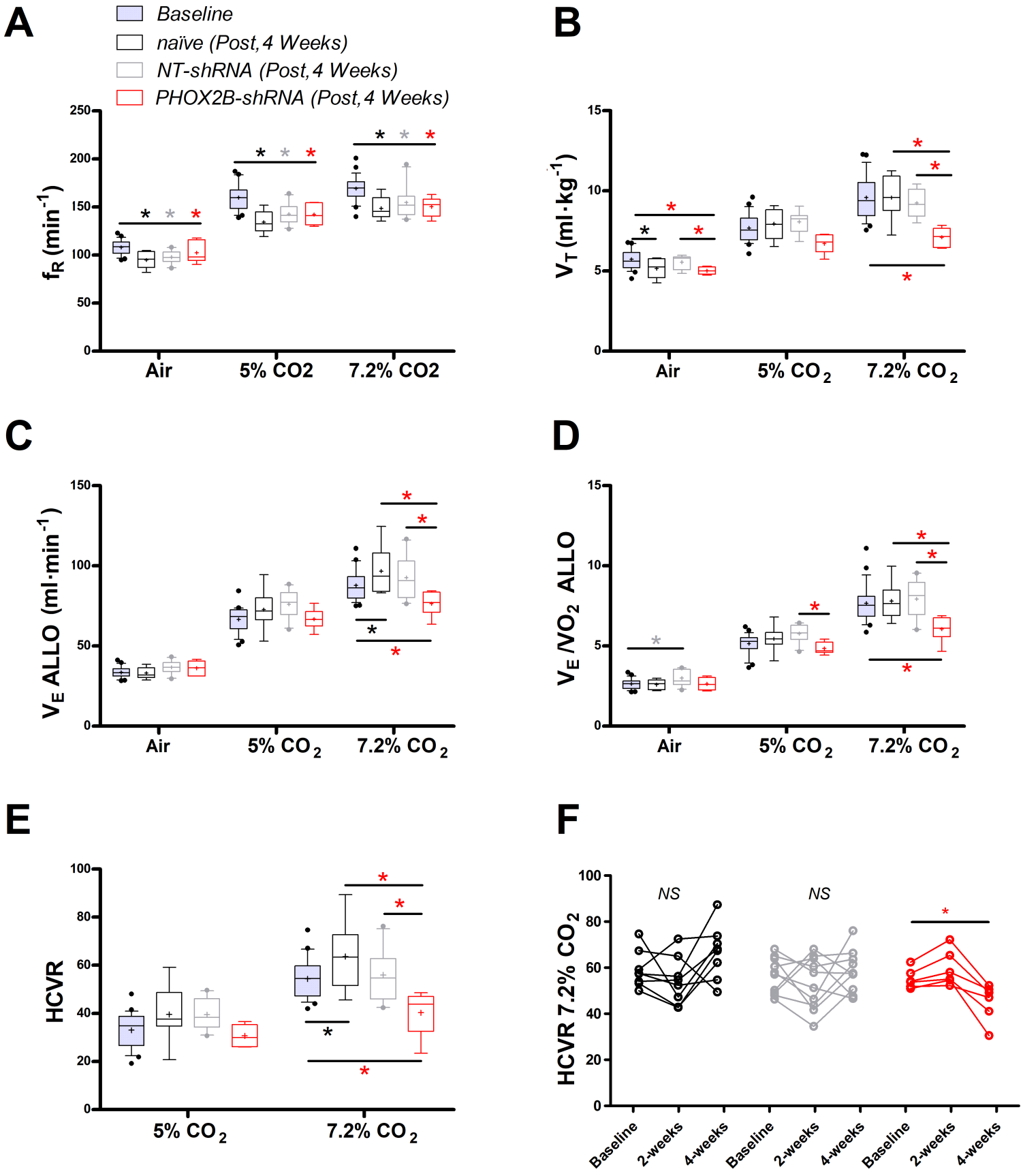
A
Baseline
naïve (Post, 4 Weeks)
NT-shRNA (Post, 4 Weeks)
PHOX2B-shRNA (Post, 4 Weeks)
f_R (min^{-1})
Air
5% CO2
7.2% CO2
B
V_T (ml·kg^{-1})
Air
5% CO_2
7.2% CO_2
C
V_E ALLO (ml·min^{-1})
Air
5% CO_2
7.2% CO_2
D
V_E /VO_2 ALLO
Air
5% CO_2
7.2% CO_2
E
HCVR
5% CO_2
7.2% CO_2
F
HCVR 7.2% CO_2
NS
NS
Baseline
2-weeks
4-weeks
Baseline
2-weeks
4-weeks
Baseline
2-weeks
4-weeks

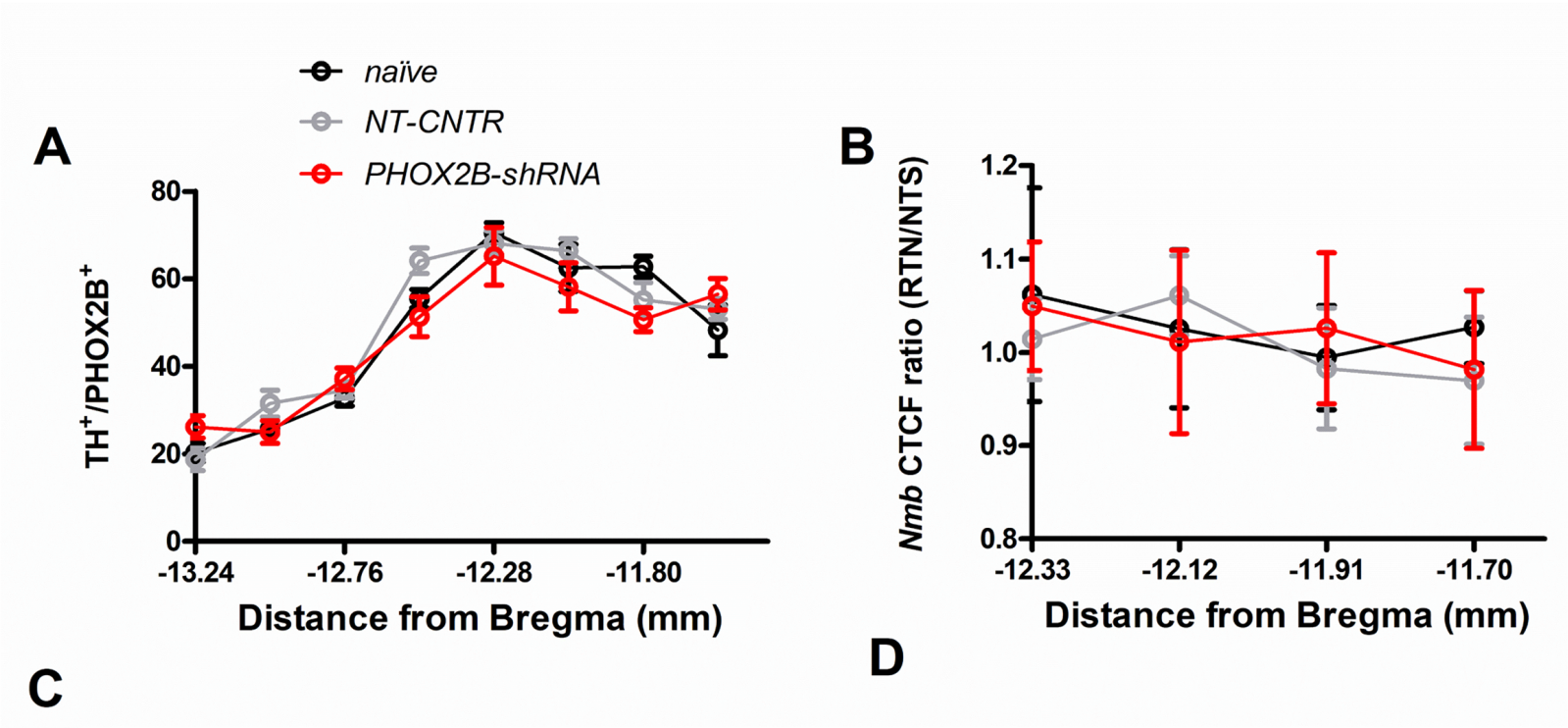
A
naïve
NT-CNTR
PHOX2B-shRNA
TH+/PHOX2B+
0
20
40
60
80
-13.24
-12.76
-12.28
-11.80
Distance from Bregma (mm)
B
Nmb CTCF ratio (RTN/NTS)
0.8
0.9
1.0
1.1
1.2
-12.33
-12.12
-11.91
-11.70
Distance from Bregma (mm)

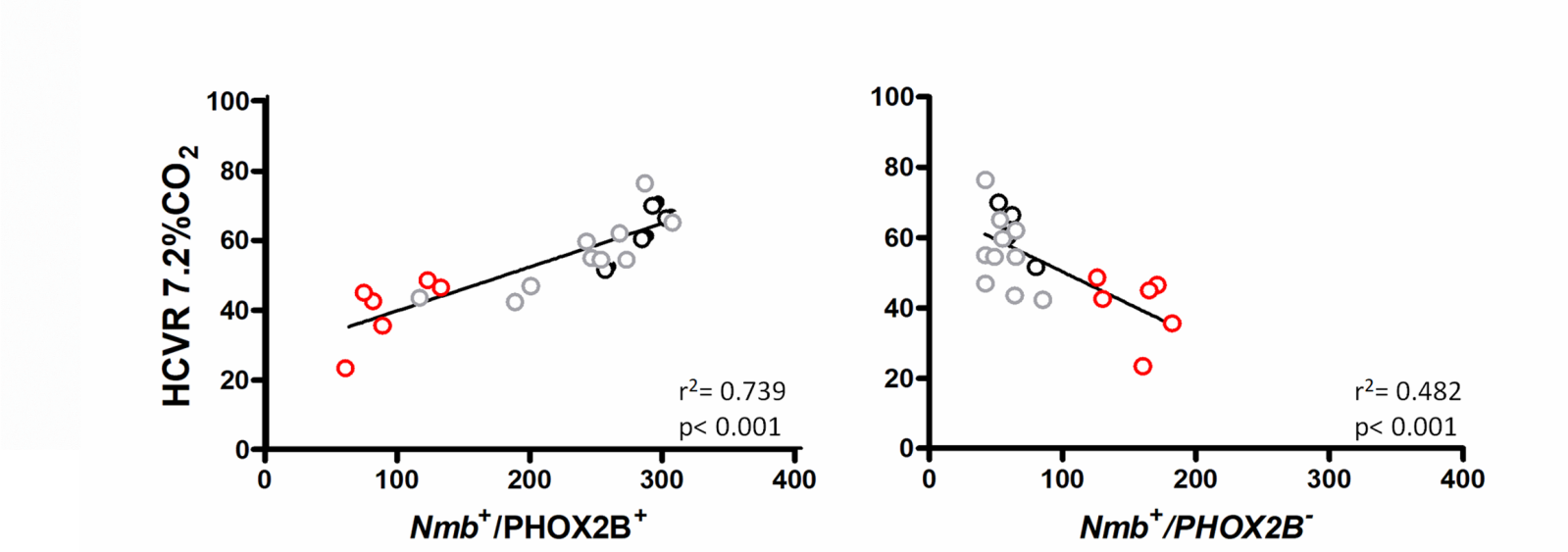
C
HCVR 7.2%CO2
0
20
40
60
80
100
0
100
200
300
400
r2= 0.739
p< 0.001
Nmb+/PHOX2B+
D
0
20
40
60
80
100
0
100
200
300
400
r2= 0.482
p< 0.001
Nmb+/PHOX2B-

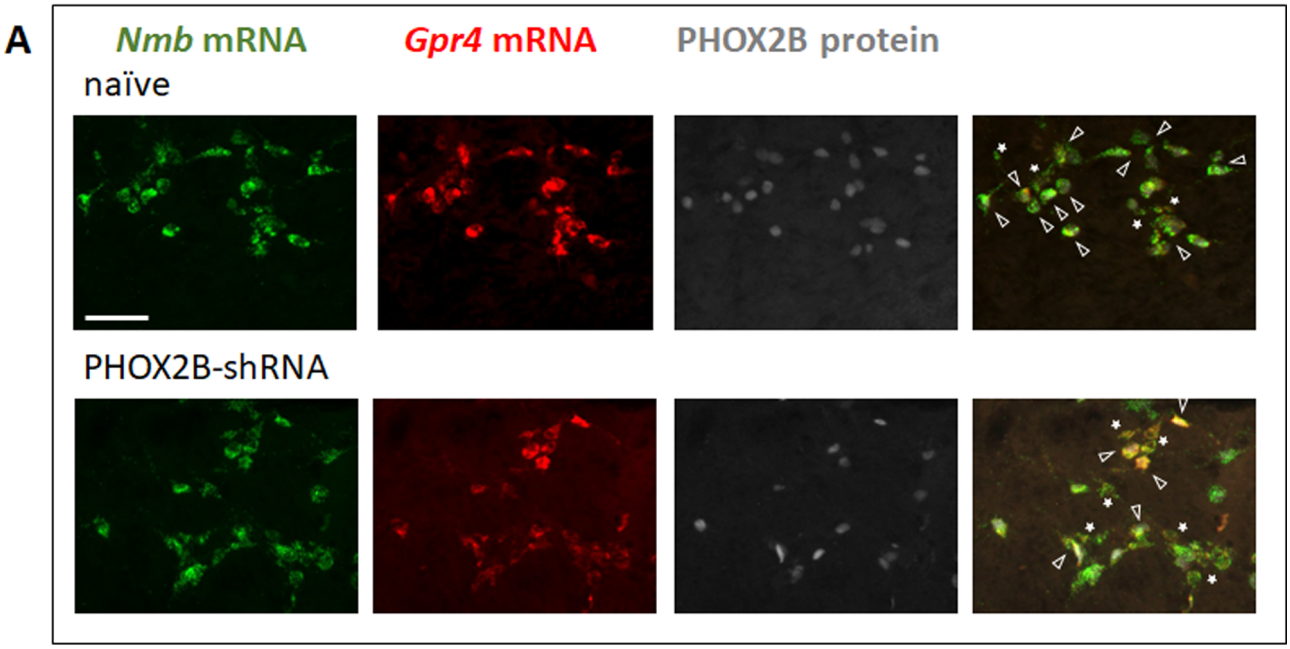
A
Nmb mRNA
Gpr4 mRNA
PHOX2B protein
naïve
PHOX2B-shRNA

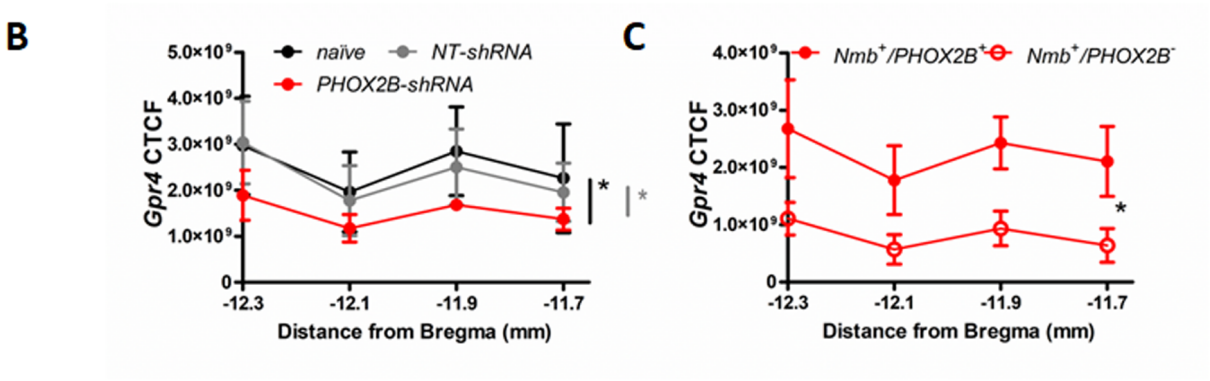
B
naïve
NT-shRNA
PHOX2B-shRNA
Gpr4 CTCF
5.0×10⁹
4.0×10⁹
3.0×10⁹
2.0×10⁹
1.0×10⁹
0
-12.3
-12.1
-11.9
-11.7
Distance from Bregma (mm)
C
Nmb⁺/PHOX2B⁺
Nmb⁺/PHOX2B⁻
Gpr4 CTCF
4.0×10⁹
3.0×10⁹
2.0×10⁹
1.0×10⁹
0
-12.3
-12.1
-11.9
-11.7
Distance from Bregma (mm)

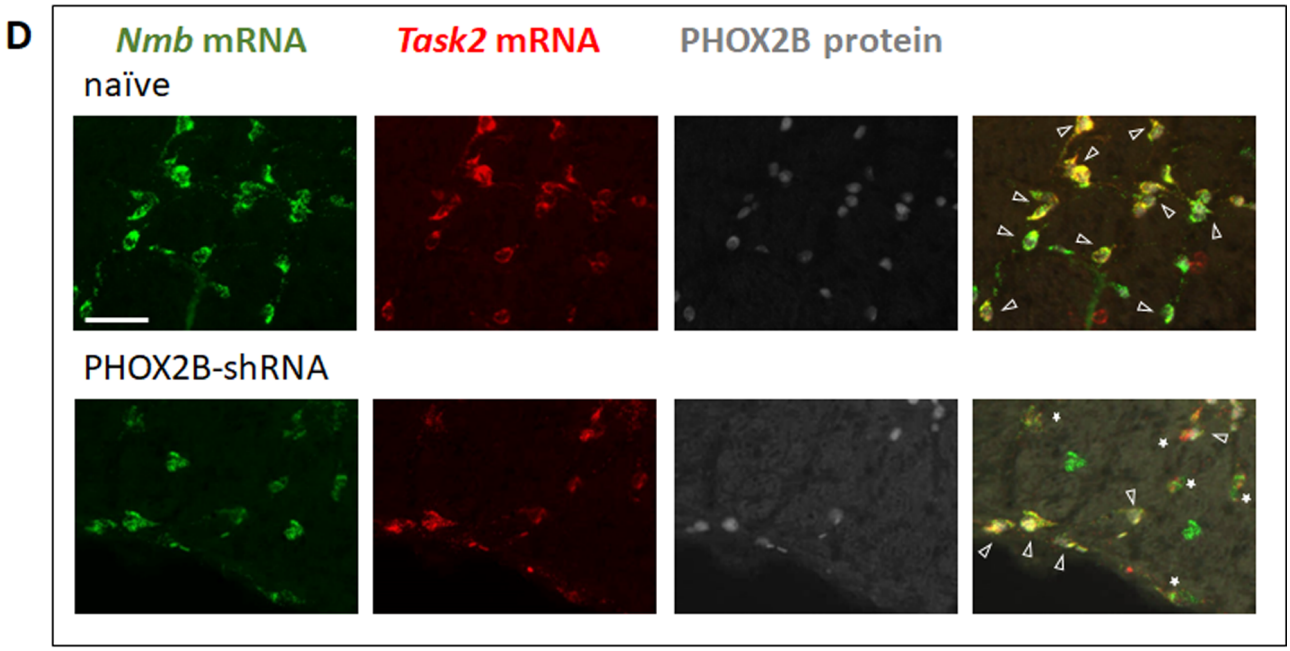
D
Nmb mRNA
Task2 mRNA
PHOX2B protein
naïve
PHOX2B-shRNA

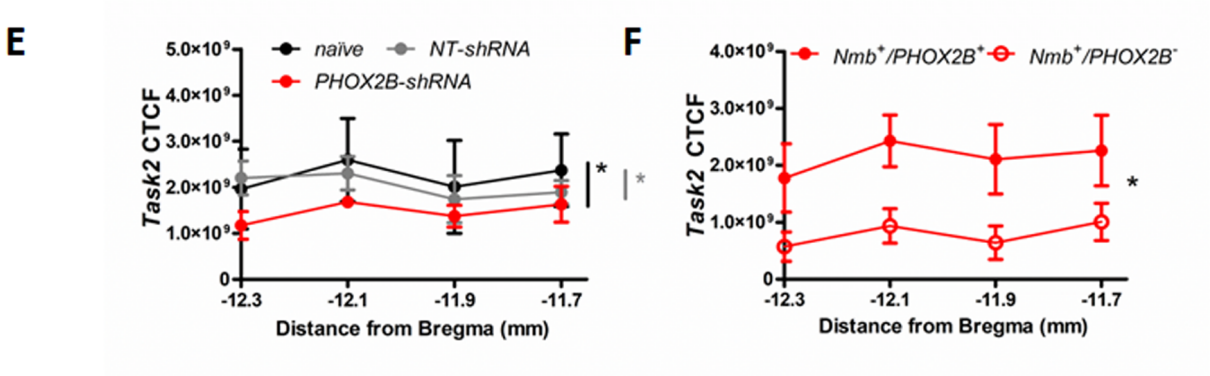
E
naïve
NT-shRNA
PHOX2B-shRNA
Task2 CTCF
5.0×10⁹
4.0×10⁹
3.0×10⁹
2.0×10⁹
1.0×10⁹
0
-12.3
-12.1
-11.9
-11.7
Distance from Bregma (mm)
F
Nmb⁺/PHOX2B⁺
Nmb⁺/PHOX2B⁻
Task2 CTCF
4.0×10⁹
3.0×10⁹
2.0×10⁹
1.0×10⁹
0
-12.3
-12.1
-11.9
-11.7
Distance from Bregma (mm)